DOKUZ EYLÜL UNIVERSITY

GRADUATE SCHOOL OF NATURAL AND APPLIED SCIENCES

SYNTHESIS AND SPECTROSCOPIC CHARACTERISATION OF Y-SHAPED FLUOROPHORES WITH AN IMIDAZOLE CORE CONTAINING N-ARYL-AZA-CROWN ETHER

by

Dilek BAYRAMİN

July, 2014

İZMİR

SYNTHESIS AND SPECTROSCOPIC CHARACTERISATION OF Y-SHAPED FLUOROPHORES WITH AN IMIDAZOLE CORE CONTAINING N-ARYL-AZA-CROWN ETHER

A Thesis Submitted to the

Graduate School of Natural and Applied Sciences of Dokuz Eylül University

In Partial Fulfillment of the Requirements for the Degree of Master of Science

in Chemistry Program

by

Dilek BAYRAMİN

July, 2014

İZMİR

M.Sc THESIS EXAMINATION RESULT FORM

We have read the thesis entitled **"SYNTHESIS AND SPECTROSCOPIC CHARACTERISATION OF Y-SHAPED FLUOROPHORES WITH AN IMIDAZOLE CORE CONTAINING N-ARYL-AZA-CROWN ETHER"** completed by **DİLEK BAYRAMİN** under supervision of **ASSOC. PROF. DR. GÜLSİYE ÖZTÜRK** and we certify that in our opinion it is fully adequate, in scope and in quality, as a thesis for the degree of Master of Science.

Assoc. Prof. Dr. Gülsiye ÖZTÜRK

Supervisor

Prof. Dr. Hüseyin Anıl

(Jury Member)

Yrd. Doç. Dr. Muhittin Aygün

(Jury Member)

Prof.Dr. Ayşe OKUR

Director

Graduate School of Natural and Applied Sciences

ACKNOWLEDGMENTS

I would like to thank my superviser, Assoc. Prof. Dr. Gülsiye ÖZTÜRK for her supports, guidance, patience, understanding and helps at the all time of my thesis. She gave me great courage to start this thesis and so I could end this study thanks to her.

I want to thank Prof. Dr. Serap ALP for her encouragement, wisdom and not letting me give up. She was always generous, thoughtful and kind to me. I am extremely grateful to her.

I place on record, my sincere gratitude to Dokuz Eylül University for the financial support with the research project 2012.KB.FEN.015.

I cannot express myself enough to thank my friend, Seher AYDIN who gave me the strength to hold on at during this study and I would like to thank her for being with me all the time.

Finally, I wish to express my thanks my family for helping me survive all the stress and their endless encouragement, supports and helps.

Dilek BAYRAMİN

SYNTHESIS AND SPECTROSCOPIC CHARACTERISATION OF Y-SHAPED FLUOROPHORES WITH AN IMIDAZOLE CORE CONTAINING N-ARYL-AZA-CROWN ETHER

ABSTRACT

In this study, two new Y-shaped fluorophores which are called as 1a and 1b were synthesized. 2a and 2b were synthesized as preliminary and then they reacted with 4-formylbenzo-aza-15-crown-5 to obtain the two Y-shaped fluorophores. The intermediate, 4-formylbenzo-aza-15-crown-5 was synthesized with Vilsmeier-Haack reaction. The Y-shaped fluorophores containing N-phenyl-aza-15-crown-5 and an imidazole core have been purified by column chromatography and precipitation processes. The structures of the synthesized compounds were characterized by using FT-IR and 1H-NMR techniques. The photophysical responses of these derivatives obtained have been determined by performing absorption with UV-vis spectrophotometer and emission measurements with fluorescence spectrophotometer. The photophysical properties of the derivatives such as absorption and emission maxima, Stokes shifts, quantum yields and photostabilities were investigated in six different solvents. The two compounds exhibited absorption maxima in the UV-vis region and emission maxima in the visible region. Both Y-shaped derivatives exhibited excellent photostability in all the solvents tested.

Keywords: Imidazole, 15-crown-5, Y-shaped fluorophore.

N-ARİL-AZA-TAÇ ETER İÇEREN İMİDAZOL ESASLI Y-ŞEKİLLİ FLOROFORLARIN SENTEZİ VE SPEKTROSKOPİK KARAKTERİZASYONLARI

ÖZ

Bu çalışmada 1a ve 1b olarak adlandırılan iki yeni Y-şekilli florofor sentezlenmiştir. 2a ve 2b başlangıç olarak sentezlenmiştir ve daha sonra iki Y-şekilli floroforu elde etmek için 4-formilbenzo-aza-15-taç-5 ile reaksiyona girmiştir. 4-formilbenzo-aza-15-taç-5 ara ürünü Vilsmeier-Haack reaksiyonu ile sentezlenmiştir. N-fenil-aza-15-taç-5 ve imidazol halkasına sahip bu iki Y-şekilli florofor kolon kromatografisi ve çöktürme işlemleri gerçekleştirilerek saflaştırılmıştır. Sentezlenen bileşiklerin yapıları FT-IR ve 1H-NMR teknikleri kullanılarak aydınlatılmıştır. Elde edilen türevlerin fotofiziksel yanıtları UV-vis spektrofotometre ile absorpsiyon ve floresans spektrofotometre ile de emisyon ölçümleri gerçekleştirilerek belirlenmiştir. Türevlerin absorpsiyon ve emisyon maksimumları, Stokes kaymaları, kuantum verimleri ve fotokararlılıkları gibi fotofiziksel özellikleri altı farklı çözücüde incelenmiştir. Bu iki bileşik UV-vis bölgesinde absorpsiyon maksimumları ve görünür bölgede emisyon maksimumları göstermişlerdir. Her iki Y-şekilli türevler çalışılan tüm çözücüler içerisinde mükemmel fotokararlılık göstermişlerdir.

Anahtar kelimeler: İmidazol, 15-taç-5, Y-şekilli florofor.

CONTENTS

Page

LIST OF FIGURES

Page

LIST OF TABLES

Page

CHAPTER ONE
INTRODUCTION

1.1 Fluorescence

The emission of light at a longer wavelength by a substance as the result of the absorption of light or other electromagnetic radiation is called fluorescence. Fluorescence is a particular type of luminescence. Fluorescence occurs in sample of gaseous, liquid and solid chemical systems. Many molecular species can exhibit fluorescence. These types of molecules are called wavelengths substances or fluorophores. A fluorophore absorbs different wavelengths of light and can re-emit light and creates a fluorescent emission in the visible light spectrum (Chavis, 2003). The molecules which act as a fluorophore are known as chromophores, fluorescent probes, sensors or dyes. Some fluorophores are shown in Figure 1.1.

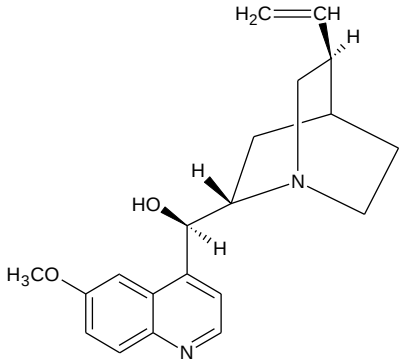

Quinine

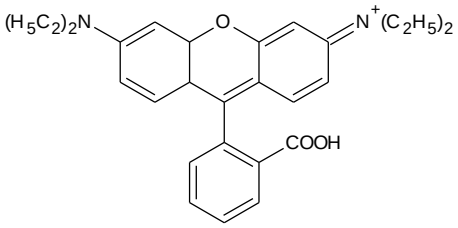

Rhodamine B

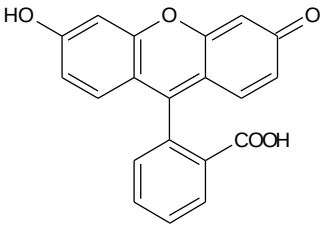

Fluorescein

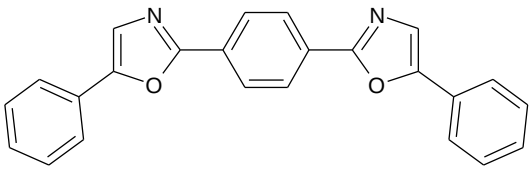

POPOP

Figure 1.1 Structures of some known fluorophores

The first known fluorophore is quinine (Figure 1.1). Quinine emits bright blue light because it has fluorescent emission peaks at around 450 nm and the UV absorption peaks at around 350 nm (Lakowicz, 1999). Quinine has well-known fluorescence quantum yield (~ 0.58 in 0.1 M sulfuric acid solution) so it is highly fluorescent and it is used as a fluorescence standard for fluorescence quantum yield measurements.

A Jabloński diagram illustrates the transitions between the electrostatic states of a molecule (Figure 1.2). Jabloński diagrams are used for discussing between the absorption and emission of light (Lakowicz, 1999).

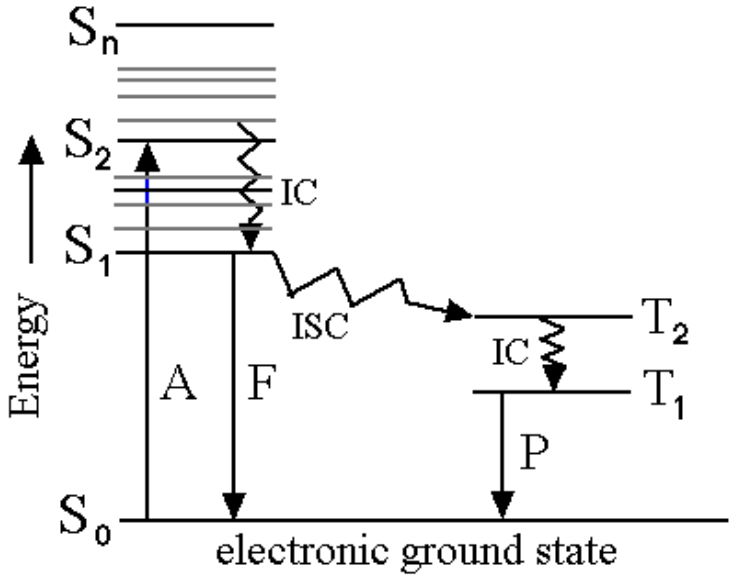

Figure 1.2 Jabloński diagram

S_0, S_1 and S_2 are the singlet electronic states; T_1 and T_2 are the triplet electronic states.

All of the molecules in a solution are in the lowest vibrational energy level of S_0 at room temperature. Absorption occurs from the lowest vibrational level of the first electronic state S_0 (fundamental electronic state) to one of the vibrational levels of S_1, S_2. The excited molecule relaxes to the lowest vibrational level of S_1 which is called an internal conversion (IC). When emission of photons happens from S_1 to S_0

this is called fluorescence. The absorbed photon energy undergoes intersystem crossing (ISC) to the first triplet state, T_1 with a spin conversion. After intersystem crossing to the first triplet state, emission from T_1 to the fundamental electronic state, S_0 is called as phosphorescence (Valeur, 2002).

1.1.1 Characteristics of Fluorophores

1.1.1.1 Stokes' Shift

Due to losing energy in the excited state because of vibrational relaxation, the fluorescence occurs at higher wavelengths than the absorption. The gap in wavelength or energy between the maximum of the first absorption band and the maximum of the emission band is termed as Stokes' shift (Figure 1.3).

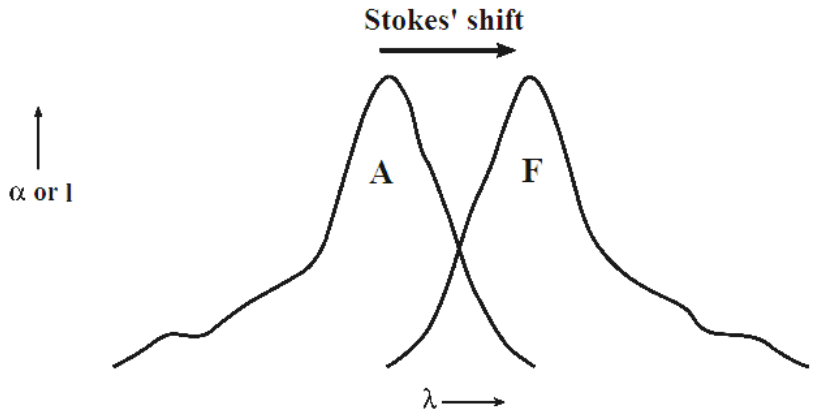

Figure 1.3 The Stokes' shift

When the dipole moment of a fluorescent molecule is higher in the excited state than in the ground state, while the polarity of solvent increases, the Stokes' shift increases too (Valeur, 2002).

1.1.1.2 Quantum Yield

The ratio of the number of emitted photons to the number of absorbed photons gives the quantum yield (or quantum efficiency) (Valeur, 2002) (Equation 1.1).

The quantum yield usually increases when the number of aromatic rings and their degree of condensation increase.

If the quantum yield is 1, all of the absorbed photons are given back with fluorescence. If the molecule doesn't show fluorescence, the quantum yield is 0.

$$\phi_F = \frac{k_F}{k_F + k_{ec} + k_{ic} + k_{isc} + k_{pd} + k_d} \quad (1.1)$$

k_F is the rate constant for fluorescence, k_{ec} is the rate constant for external conversion ($S_1 \rightarrow S_0$), k_{ic} is the rate constant for internal conversion ($S_1 \rightarrow S_0$), k_{isc} is the rate constant for intersystem crossing ($S_1 \rightarrow T_1$), k_{pd} is the rate constant for predissociation and k_d is the rate constant for dissociation (Skoog, Holler & Nieman, 1998).

1.1.1.3 Fluorescence Lifetime

The fluorescence lifetime of a molecule is defined as the average time the molecule stays in its excited state before emitting a photon.

The fluorescence lifetime of fluorescent substances is 10^{-9} - 10^{-7} s.

1.1.1.4 Fluorescence Quenching

Decreases in the intensity of fluorescence are termed as guenching and these species which cause these decreases are called as quenchers. The quenchers can turn fluorophores into nonfluorescent complexes.

If a fluorophore contacts with other molecules in solution when it is in excited state, collosional quenching occurs. Oxygen, halogens, amines and electron deficient molecules like acrylamide can act as collosional quenchers (Lakowicz, 1999).

1.2 Fluorescence and Structure

Aromatic functional groups with low energy $\pi \rightarrow \pi^*$ transition levels produce strong fluorescence. Because the $\pi \rightarrow \pi^*$ transition has high fluorescence quantum yield and high molar absorptivity according to the $n \rightarrow \pi^*$ transition. Some compounds which have aliphatic and alicyclic carbonyl groups or highly conjugated structures may also show fluorescence.

For example, the linear aromatic hydrocarbons such as naphthalene, anthracene, naphthacene and pentacene (Figure 1.4) can emit light in the ultraviolet region like blue, green and red, respectively (Valeur, 2002).

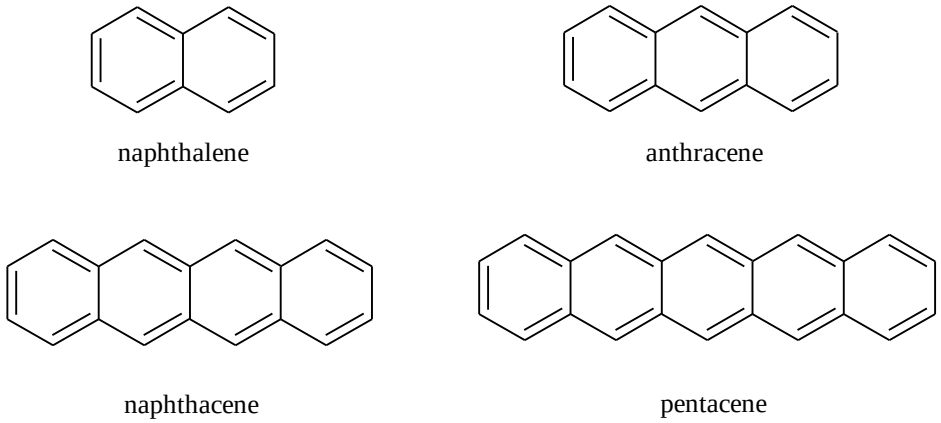

Figure 1.4 Linear aromatic hydrocarbons

Even though they are aromatic, there are some compounds which do not show fluorescence. Compounds containing heteroatoms such as pyridine, furan, thiophene, pyrrole (Figure 1.5) can lead to unwanted $n \rightarrow \pi^*$ transitions and do not show fluorescence.

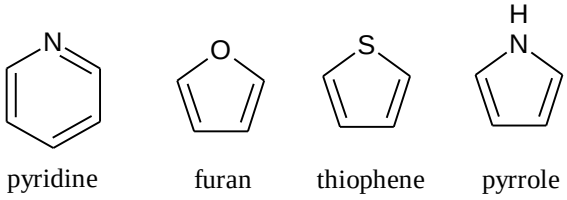

Figure 1.5 Non-fluorescent compounds

Fused aromatic systems exhibit fluorescence very well, because these molecules have high molar absorptivity values. Compounds such as quinoline, isoquinoline and indole (Figure 1.6) show intense fluorescence. Even though the heterocyclic nitrogen atom has lowest energy $n \rightarrow \pi^*$ transitions which cause low quantum yields and inhibit fluorescence, fusion of a heterocyclic unit to benzene rings leads to increase the molar absorptivity of the absorption peak. Thus the lifetime of the excited state is shorter and they show strong fluorescence (Skoog, Holler & Nieman, 1998).

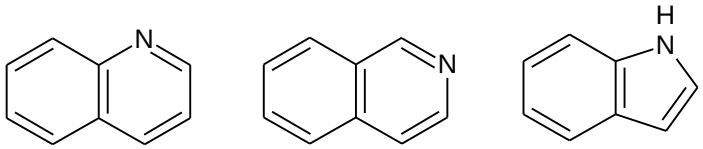

quinoline isoquinoline indole

Figure 1.6 Azarenes

Substitution on the benzene ring affects the wavelength of absorption maxima and changes the fluorencence efficiency. Substitution with electron donating groups, such as an amine and a hydroxyl group enhance the molar absorption coefficient and cause an increase in fluorescence. Substitution with electron withdrawing groups, such as a carboxylic acid, nitro, carbonyl group and an aldehyde group decrease or inhibit fluorescence. Because the energy of the $n \rightarrow \pi^*$ state is less than that of the $\pi \rightarrow \pi^*$ state. Substitution of a halogen group decreases the fluorescence because of intersystem crossing to the triplet state. This effect increases with increasing atomic number of halogen and it is called as heavy atom effect (Skoog, Holler & Nieman, 1998).

Rigid molecules lead to lower rate constants for internal and external conversion, thus they have high quantum yields. For example, quantum yields for fluorene and biphenyl (Figure 1.7) are 1.0 and 0.2, respectively (Skoog, Holler & Nieman, 1998).

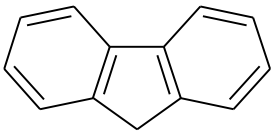

fluorene

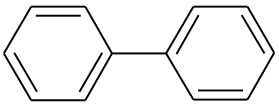

biphenyl

Figure 1.7 Rigid molecules

When rigid molecules are complexed with a metal ion, it reduces the internal conversion rate (k_{ic}) and it causes an increase in fluorescence intensity. For example, the fluorescence intensity of the zinc complex of 8-hydroxyquinoline (Figure 1.8) is much more than the fluorescence intensity of 8-hydroxyquinoline (Skoog, Holler & Nieman, 1998).

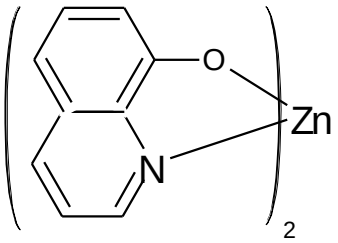

Figure 1.8 The zinc complex of 8-hydroxyquinoline

1.3 Fluorescent Probes and Sensors

Fluorescent molecules are really useful for detection in many applications because of their great selectivity and sensitivity. So these molecules can act as probes and they are called as fluorescent probes. They can be used for investigation of physicochemical, biochemical and biological systems. For instance, probes can covalently attach to proteins, polynucleotides, phospholipids, polymer chains, surfactants, etc. Therefore they are tagged and detected by these probes.

Fluorescent sensors are used in many applications for analytical chemistry, medicine, clinical biochemistry, the environment, etc.

Many cations (H^+, Li^+, Na^+, K^+, Ca^{2+}, Mg^{2+}, Zn^{2+}, Pb^{2+}, Al^{3+}, Cd^{2+}, etc.), anions (halide ions, carboxylates, citrates, etc.), neutral molecules (sugar, etc.), gases (O_2, CO_2, NO, etc.), biochemical analytes (amino acids, coenzymes, carbohydrates, nucleosides, nucleotides, etc.) can be detected by fluorescent sensors. The fluorescent sensors also can be used for optical fibers (Valeur, 2002).

Detecting cations have a great importance for clinical biochemists and biologists. Some biological processes like transmission of nerve impulses, regulation of cell activity, muscle contraction require cations like sodium, potassium, calcium and magnesium, etc. Diagnosis requires detection of metal ions such as Li^+, Na^+, K^+, Ca^{2+}, Mg^{2+} in blood and this process is very useful in medicine (Valeur, 2002).

Anions also can be detected by fluorescent molecules like cations. The detection of anions is very important because of anionic pollution in ground water like nitrates and phosphates, the roles in human biology and disease regulation like the chloride ion (Valeur, 2002).

The complex formation, redox reactions, substitution reactions and guenching are used for the processes of anion detection with fluorescence sensing (Fernandez & Muñoz de la Peña, 1985).

1.4 Imidazole

1.4.1 The Structure and Properties

Imidazole was first synthesized by Heinrich Debus in 1858. It is a planer five-membered heterocyclic ring which has two nitrogen atoms as heteroatoms at 1st and 3rd positions (Figure 1.9). Imidazole is a member of 1,3-diazoles. Imidazole derivatives are known as imidazoles.

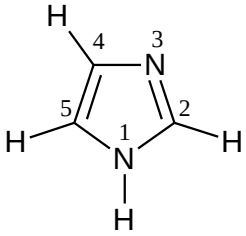

Figure 1.9 Imidazole (glyoxaline, 1,3-diazole or 1,3-diazacyclopenta-2,4-diene)

Imidazole has two tautomeric forms. The tautomeric forms are equivalent and locate at 4 and 5 positions (Figure 1.10).

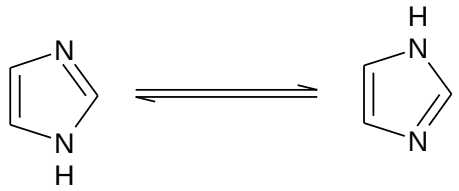

Figure 1.10 The tautomeric forms of imidazole

Imidazole is an amphoteric compound which means that it can act as both an acid and as a base.

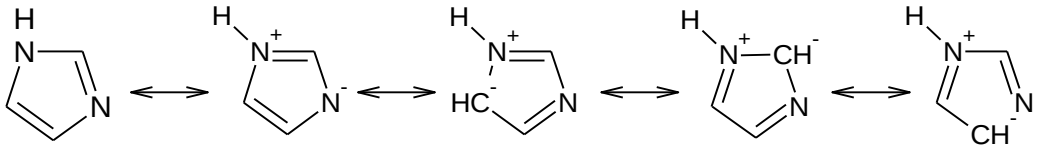

Figure 1.11 The resonance structures of imidazole

Imidazole is a base with sp^2 hybridized nitrogen atom (pK_a 7.0), N-3 atom is the basic side. When it is protonated on N-3 atom, it gives the imidazolium cation. Imidazole is an acid with sp^3 hybridized nitrogen atom (pK_a 14.5) and the acidic proton is located on N-1 atom (Figure 1.11).

Imidazole has a really high polarity. Its dipole moment is 3.61 D, thus it is highly soluble in water and other polar solvents but it is not soluble in apolar solvents. The N–H proton can form the intermolecular hydrogen bonding (Bhatnagar, Sharma & Kumar, 2011).

1.4.2. Synthesis of Imidazoles

1.4.2.1 Debus Synthesis

Imidazole can be synthesized by the reaction which is between a diketone and an aldehyde in ammonia (Figure 1.12). When glyoxal and formaldehyde are used instead of diketone and aldehyde, imidazole is obtained. But this synthesis has low yields (Debus, 1858).

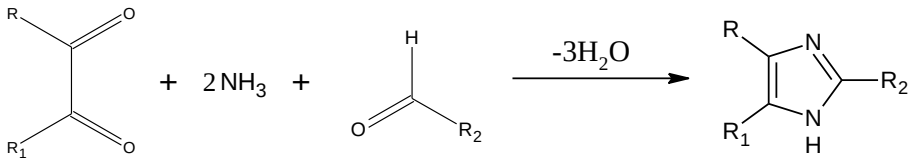

diketone ammonia aldehyde C-substituted imidazole

Figure 1.12 Formation of C-substituted imidazole from Debus reaction

1.4.2.2 Radiszewski Synthesis

Radiszewski reaction is consist of condensation of a dicarbonyl compound (benzil) and a ketoaldehyde (benzaldehyde) in the presence of ammonia in one microwave modification and this reaction forms 2,4,5-triphenylimidazole (lophine) (Crouch, Howard, Zile & Barker, 2006) (Figure 1.13).

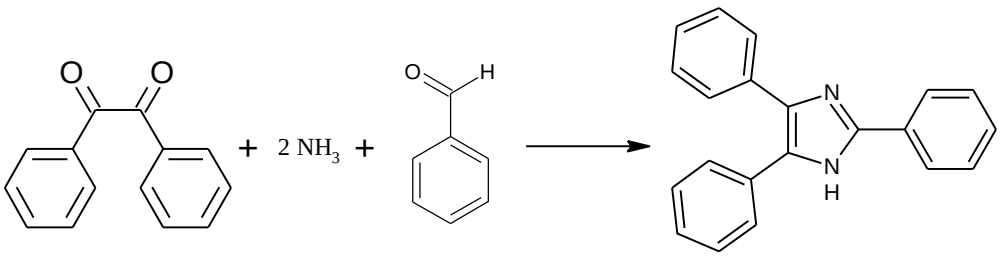

benzil benzaldehyde 2,4,5-triphenylimidazole

Figure 1.13 Formation of 2,4,5-triphenylimidazole from Radiszewski reaction

1.4.2.3 Cyclization of α-Acylaminoketones

A 2,4,5-trisubstituted imidazole can be synthesized by cyclization of an α-acylaminoketone (Finar, 2006) (Figure 1.14).

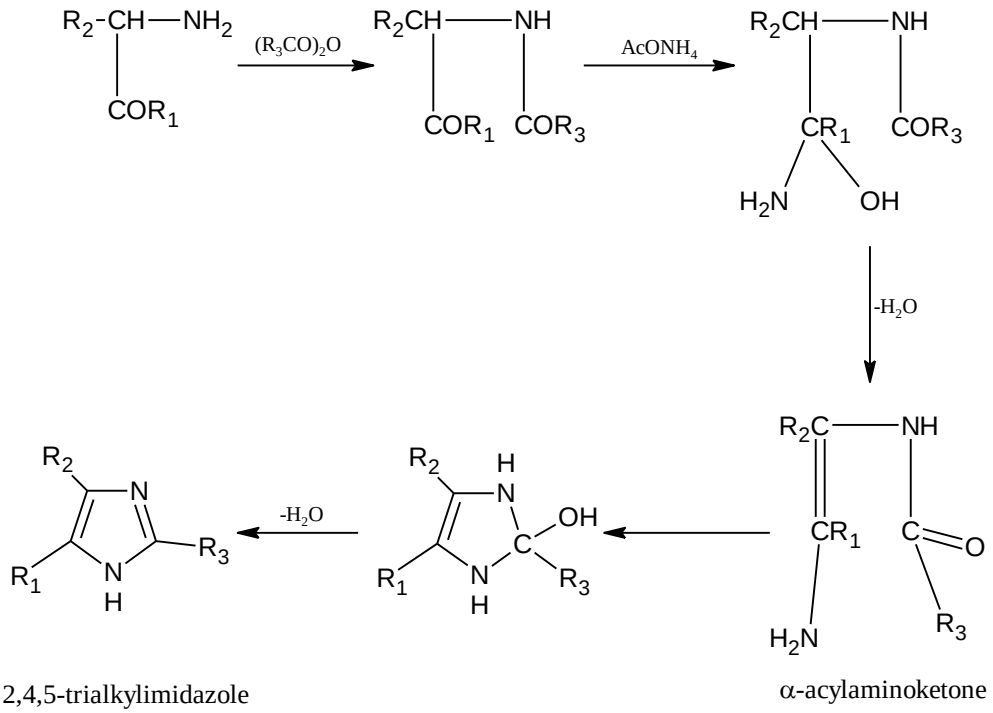

Figure 1.14 Formation of 2,4,5-trialkylimidazole from an α-acylaminoketone

1.4.2.4 With a Dehydrogenating Catalyst

A 2,4,5-trialkylimidazole can be synthesized by treating a 1,2-diaminoalkane with a carboxylic acid in the presence of a dehydrogenating catalyst like platinum on alumina at high temperatures (Figure 1.15).

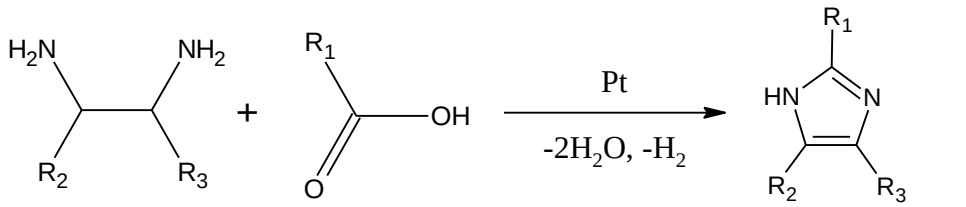

Figure 1.15 Formation of 2,4,5-trialkylimidazole with a dehydrogenating catalyst

1.4.2.5 From α-Haloketone

This reaction is between an amidine and alpha halo ketone. 2,4,5-trialkylimidazole can be obtained from the reaction (Elderfield, 1957) (Figure 1.16).

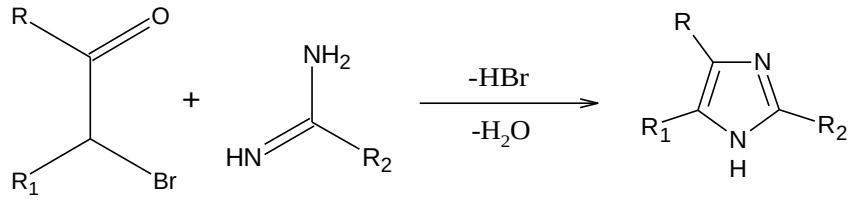

a-haloketone amidine 2,4,5-trialkylimidazole

Figure 1.16 Formation of 2,4,5-trisubstituted imidazole from α-haloketone

1.4.2.6 With a Reaction of Photolysis

Another way of synthesis of a 2,4,5-trisubstituted imidazole is a photolysis reaction of 1-vinyltetrazole (Figure 1.17).

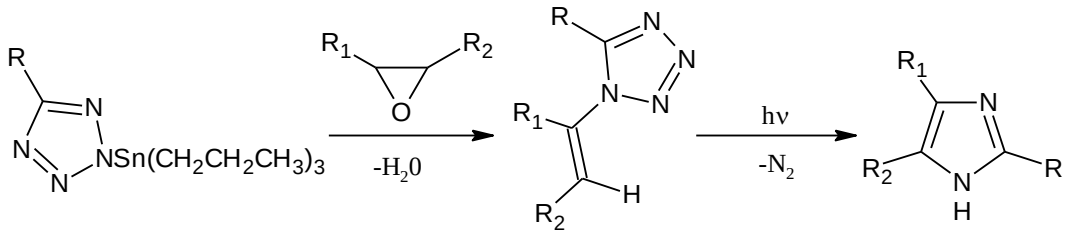

2-tributylstannyltetrazole 2,4,5-trialkylimidazole

Figure 1.17 Formation of 2,4,5-trialkylimidazole by the photolysis reaction

1.4.3 Applications of Imidazoles

Imidazole is a natural compound and exists in many important natural molecules such as the amino acid histidine, vitamin B_{12}, histamine, biotin and purines like adenine and guanine. The amino acid, histidine is an imidazole compound and presents in many proteins and enzymes and binds functions of hemoglobin. Histidine

can convert to histamine by decarboxylation. Histamine exists in many tissues of human body and has many biological effects.

Imidazole is used for the purification of his-tagged proteins in immobilised metal affinity chromatography (IMAC). The proteins bound to Ni ion attached to the surface of beads are eluted by imidazole in the chromatography column. An excess of imidazole passes through the column, displaces the his-tagged from nickel coordination and provides the his-tagged proteins free.

Imidazole is widely used for purifying processes of protein. Therefore, imidazole was used as a catalyst and chemically denatured green fluorescent protein (EGFP) (Shi et al., 2007).

Imidazoles have many important features as medicinal agents. Imidazole derivatives play many important roles in various pharmacological activities such as anticancer, antibacterial, antifungal, antiviral, anti-HIV, antitubercular and analgesic activities (Shalini, Sharma & Kumar, 2010).

The substituted imidazole derivatives participate in the class of azole antifungals which include ketoconazole, miconazole, clotrimazole and econazole (Bhatnagar, Sharma & Kumar, 2011). Many imidazoles like azomycin, clonidine, moxonidine, miconazole, clotrimazole and ergothioneine have been developed as pharmacological agents. There are many important applications of imidazole derivatives for treatment of denture stomatities (Al-Azzawi, 2007).

1,2,4,5-tetrasubstituted imidazole derivatives (Figure 1.18) have been synthesized by the reaction of purified imidazole compounds and benzyl chloride in the presence of sodium hydride by Uçucu and co-workers. The imidazole derivatives showed analgesic activity and the analgesic activity was almost equivalent to that of morphine at 1 mg / kg (Uçucu, Karaburun & Işikdağ, 2001).

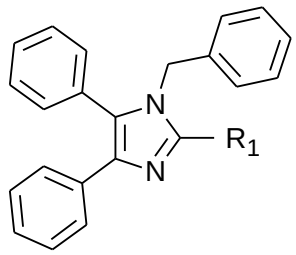

Figure 1.18 1-benzyl-2-substituted-4,5-diphenyl-1H-imidazole

Imidazole derivatives show fluorescence upon metal binding as a chelator. Thus they have important analytical applications with their fluorescence and chemiluminescence properties. Saravanan and co-workers have developed a set of imidazole derivatives as sensitive fluorescent chemisensors for transition metal ions such as Hg^{2+}, Pb^{2+} and Cu^{2+}. They showed sensitive and selective responses towards these metal ions (Saravanan, Srinivasan, Thanikachalam & Jayabharathi, 2011). Jayabharathi and co-workers have synthesized some imidazole derivatives (1 and 2) (Figure 1.19) as sensitive and selective fluorescent chemisensors for sensing and imaging of transition metal ions such as Hg^{2+}, Pb^{2+}, Cu^{2+}, Zn^{2+}, Co^{2+} and Fe^{2+}. These imidazole derivatives exhibited large hyperpolarizability values and increased transparency in the visible region. Thus they can also act as NLO materials (Jayabharathi, Thanikachalam, Srinivasan & Jayamoorthy, 2011).

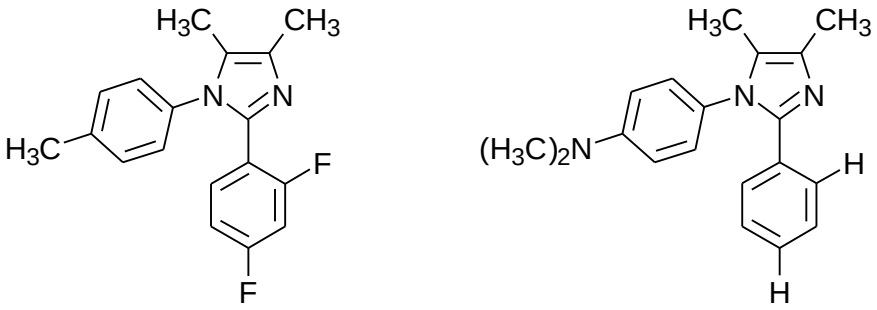

1 2

Figure 1.19 Structures of imidazole derivatives 1 and 2

Study of optical properties of five-membered nitrogen-containing heterocyclic compounds has showed that they also have an integral part of anion sensors. Zhao and co-workers have developed a series of cationic iridium (III) complex salts

containing imidazolyl substituents as chemosensors for F^-, CH_3COO^- and $H_2PO_4^-$ anions. The addition of F^-, CH_3COO^- and $H_2PO_4^-$ anions led to significant changes in UV-vis absorption and emission spectra and caused emission color changes which could be seen by naked eye (Zhao et al., 2007).

Imidazole core has been used in organic light-emitting diodes (OLEDs) applications. Islam and co-workers have synthesized two bis-imidazole derivatives (BSIB-1 and BSIB-2) (Figure 1.20) as dopant emitters in electroluminescent devices and they showed very high melting points, glass transition temperatures and emitted bright blue-green light in solution states. Because of these features, they were good dopant emitters in organic electroluminescent devices (Islam et al., 2002).

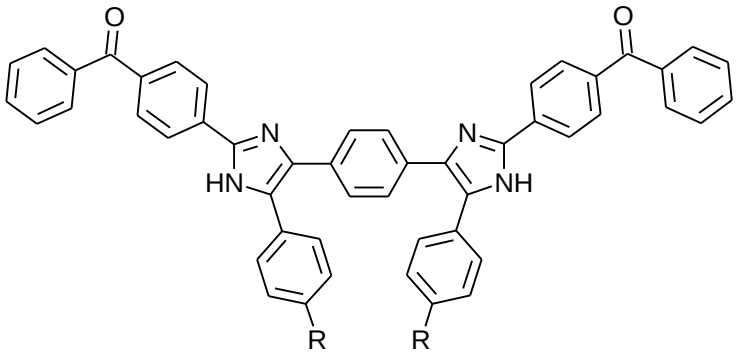

Figure 1.20 BSIB-1 (R=H) and BSIB-2 (R=Me)

Imidazole can act as a corrosion inhibitor for transition metals like copper. Corrosion inhibitor prevents the conductivity of the copper when decreasing because of corrosion in aqueous systems.

If the imidazole ring is a form of cation, it is the salt of imidazole and salts of imidazole are called as imidazolium salts, such as imidazolium chloride. When the protonation or substitution at nitrogen of imidazole, these salts are formed. These salts have been used as ionic liquids and stable carbenes. Salts of imidazole are also formed even when the imidazole ring is deprotoned and these salts are known as imidazolide or imidazolate salts, such as sodium imidazolide.

1.5 Crown Ethers

Crown ethers were discovered by Charles Pedersen in the early 1960s (Pedersen, 1967) and they are macrocyclic compounds which consist of ring structures containing a number of ether groups ($-CH_2-O-CH_2-$) in regular order.

Crown ethers have the ability of complexation with metal ions selectively. They are able to bind inorganic ions, organic ions and neutral species. But especially they have greatest affinity for the alkali (M^+) and alkaline earth (M^{2+}) cations (Steed, 2001). They are known as spesific cation binding agents. They have the ability of complexation with metal ions selectively. Thus a process with 18-crown-6 has been developed for the separation of strontium from acidic nuclear waste streams (Draye et al., 1997).

Some oxygen atoms in crown ethers can be replaced by nitrogen atoms to form aza-crown ethers. Crown ethers are also able to form complexes strongly with alkali, alkaline earth and heavy metal cations. On the other hand the aza-crown ethers have better complexing ability for transition metal ions than all-oxygen crown compounds. Minkin and co-workers have designed a kind of chromogenic and fluorescent chemosensors containing crown-, azacrown-, and thiacrown-ether. They have found that crown ether-based chemosensors (CEBC) could be used for detection of alkali and alkaline earth metal cations and monitoring various analytes in many studies (Minkin, Dubonosov, Bren & Tsukanov, 2008).

N-aryl-aza-crown ether derivatives can show fluorescence properties because of the fluorescent aryl which covalently bound to the nitrogen of an aza-crown ether. By changing intensity of the signal of the fluorophore, N-aryl-aza-crown ethers are able to act as sensitive and selective sensors toward cations. Therefore, Yu and co-workers have developed two stilbene derivatives; CN-crown and H-crown containing monoaza-15-crown-5 (Figure 1.21) as fluorescent chemosensors which were sensitive and selective toward Li^+ and Fe^{3+} toxic metals. While the H-crown selectively recognized Li^+ and Fe^{3+} by fluorescence quenching, the CN-crown

showed high selectivity and sensitivity toward Li^+ only. The CN-crown was quenched only by Li^+ (Yu, C. Y. Chen & Y. Chen, 2011).

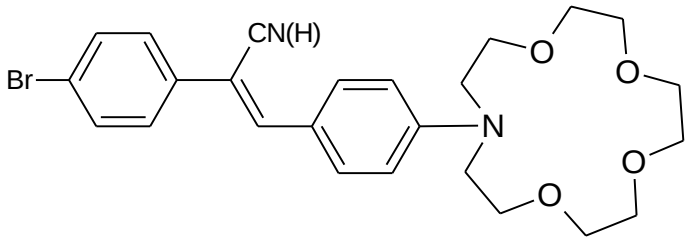

Figure 1.21 CN (H)-crown

Ozturk and co-workers have synthesized 5-oxazolone derivatives which have N-phenyl-aza-15-crown-5 (Figure 1.22) and they showed high absorption and emission maxima in the visible region. All the derivatives can be used as probes for biological applications (Ozturk, Alp & Ergun, 2007).

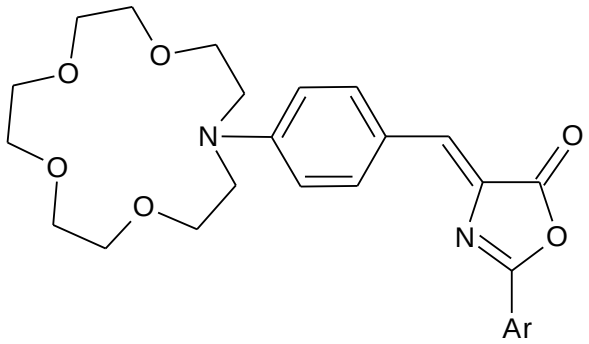

Figure 1.22 5-oxazolone derivatives containing N-phenyl-aza-15-crown-5

Pond and co-workers have designed chromophores which have a donor-acceptor-donor structure and one or two mono-aza-15-crown-5 moieties and it has been found that had a large two-photon absorption cross-section value. When aza-crown nitrogen atoms have bound Mg^{2+}, it caused a blue shift and the two-photon absorption cross section was decreased. Because of these changes, these chromophores can be used as two photon excited metal sensing fluorophores (Pond et al., 2004).

1.6 Y-shaped Fluorophores

Second order nonlinear optical (NLO) materials have great interest in various important applications such as two-photon absorbing materials, opto-electronics, photonics and organic light-emitting diodes (He, Tan, Zheng & Prasad, 2008; Kim, Ju, Park, Do & Lee, 2008) because of their large first hyperpolarizability (β), high thermal stability, good optical transparency in the visible region, good miscibility with high performance polymers and excellent solubility.

Santos and co-workers have synthesized heterocyclic imidazole based Y-shaped NLO chromophores which have long conjugation pathways. Thiophene was used to have these systems improved molecular nonlinearity and nitro groups were attached to the phenyl end without compromising thermal stability. As a result, a new series Y-shaped NLO imidazoles which have enhanced molecular nonlinearity, high thermal stability, excellent solubility and good transparency have been obtained with condensation of 2-formylthiophene and benzil derivatives in the presence of ammonium acetate (Santos et al., 2001). Wang and co-workers have developed four NLO chromophores which contain multiple donor and acceptor groups and an imidazole ring as Y-shaped molecules. The structures possess high thermal stability, good transparency and non-linearity. However, a feature of these chromophores is that they can bond to a polymeric or inorganic backbone chemically (Wang, Zhao, Xu, Wu & Cheng, 2002). Ren and co-workers have synthesized two second order Y-shaped NLO chromophores and one of them contains thermally stable an imidazole core and multiple donor or acceptor substituents (Figure 1.23). The chromophores exhibited improved nonlinearity-transparency-thermal stability trade off (Ren, Wang, Wu, Xu & Dong, 2008).

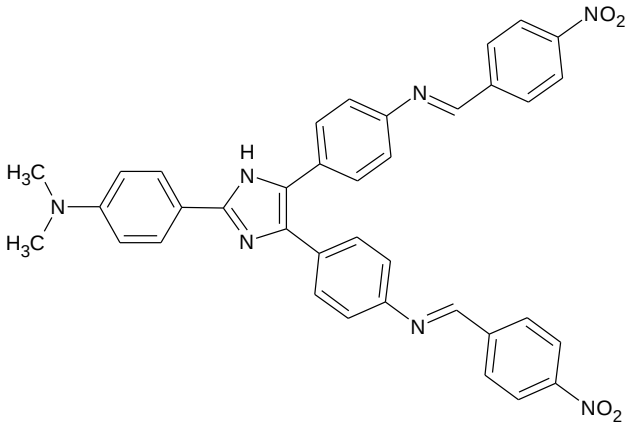

Figure 1.23 The Y-shaped NLO chromophore containing an imidazole ring

Imidazole derivatives can be used as sensitive fluorescent chemisensors due to their fluorescence properties and they can sense and image by binding metal ions, thus they can make sensible fluorescence changes. As a result, many imidazole derivatives have been used as a sensor. Ozturk and co-workers have synthesized four imidazole based Y-shaped NLO fluorophores from the reaction of 1,6-bis(2,4,6-trimethoxyphenyl)hexa-1,5-diene-3,4-dione and four different aldehydes; 1. Ar: 4-cyanophenyl, 1:1a; 2. Ar: phenyl, 1:1b; 3. Ar: 9-anthryl, 1:1c; 4. Ar: 4-nitrophenyl, 1:1d (Figure 1.24). These derivatives exhibited large Stokes' shift values, excellent photostabilities and intense emission maxima in the visible region. These features showed that these derivatives can be designed as fluorescent sensors (Ozturk, Karakas, Karadag & Yorgun, 2012).

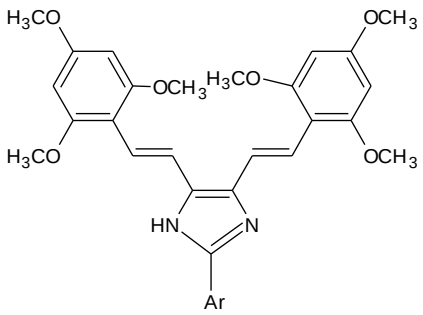

1

Figure 1.24 Structure of imidazole based Y-shaped NLO fluorophores

Three Y-shaped molecules containing an imidazole ring have been designed as highly sensitive chemisensors for transition metal ions such as Hg^{2+}, Pb^{2+} and Cu^{2+} by Jayabharathi and co-workers. The chemisensors showed good transparency in the visible region (Jayabharathi, Thanikachalam, Devi & Srinivasan, 2011). A Y-type fluorophore (*E,E*'-4,4'-[(2,2'-bis(ethene-2,1-diyl)dibenzoate)-(2-(4-(methoxycarbonyl)phenyl)-1*H*-imidazole-4,5-diyl) (1) has been developed as a ratiometric fluorescent sensor for fluoride anion (F^-) because of its health and environmental issues by Zhang and co-workers. The fluorophore (1) was synthesized as a two-photon excited fluorescence (TPEF) sensor which is highly selective for fluoride anion. When the TPEF-sensor reacted with fluoride anion, an emission color change occurred from green to brown which could be seen by naked-eye (Zhang et al., 2008) (Figure 1.25).

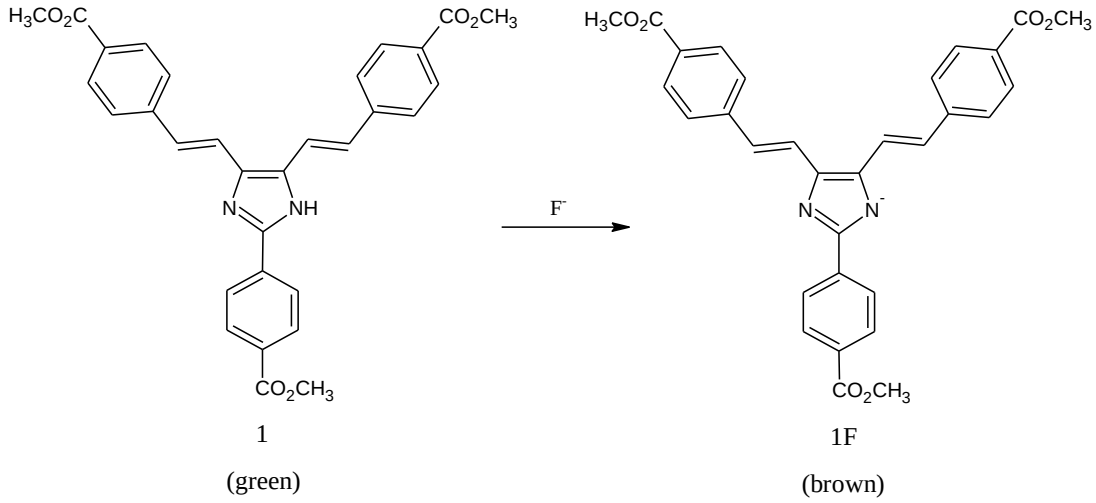

Figure 1.25 The deprotonation reaction between 1 and 1F

In another work, Zhang and co-workers have synthesized a Y-type fluorophore (FD3) containing an imidazole ring, 4-(methylbenzoate)phenylethenyl group as the two branches and an electron-withdrawing group of 4-formylphenyl at the other branch, as a two-photon excited fluorescence (TPEF) sensor. The fluorophore (FD3) showed intense TPEF which has a large two-photon absorption cross section of more than 9000 GM and exhibited high selectivity for cysteine (cys) and homocysteine (hcy). When the -CHO group of FD3 reacted with cys, a fluorescent color change was observed from green to cyan (Zhang et al., 2007) (Figure 1.26).

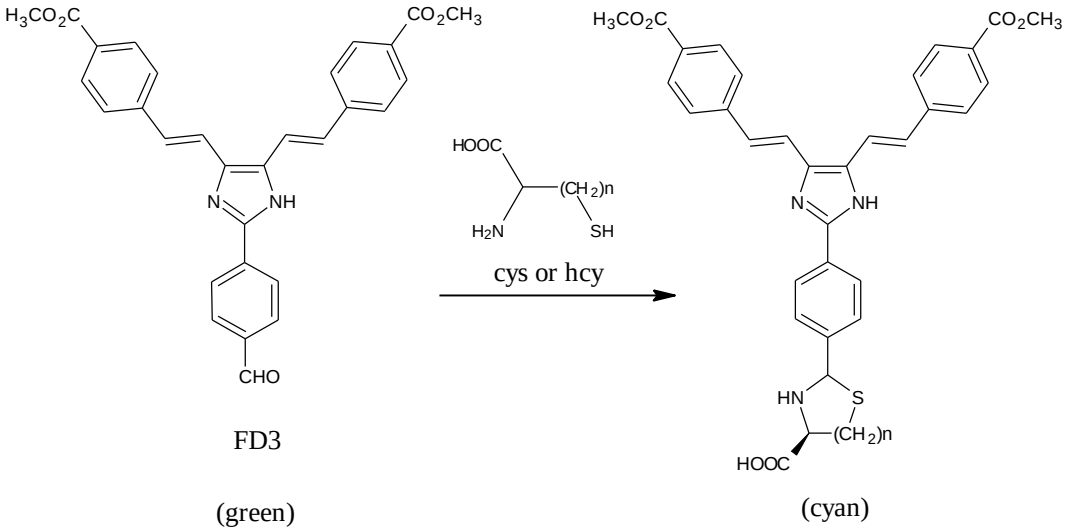

Figure 1.26 The possible reaction of FD3 with cys or hcy

Boni and co-workers have developed three different sulfonyl based Y-shaped molecules containing an imidazole-thiazole core. These molecules showed large two- and three-photon absorption (2PA and 3PA) cross sections and so they can be used as fluorescent probes for two- and three-photon microscopy (Boni et al., 2005). Karunakaran and co-workers have developed an imidazole derivative, 4,5-diphenyl-2(E)-styryl-1H-imidazole (Figure 1.27). This derivative showed selective fluorescence enhancement by sensing of nanocrystalline TiO_2 rutile and so it can be used for deduction and estimation of rutile TiO_2 nanoparticles (Karunakaran, Jayabharathi, Jayamoorthy & Devi, 2012).

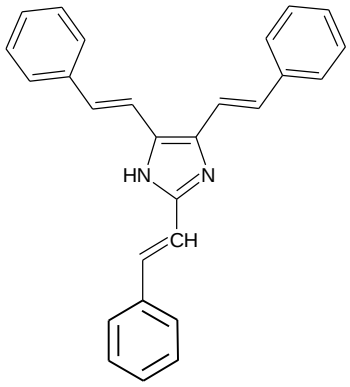

Figure 1.27 4,5-diphenyl-2(E)-styryl-1H-imidazole

CHAPTER TWO
MATERIALS AND METHODS

2.1 Materials

4-methoxybenzaldehyde, 4-nitrobenzaldehyde, 4-cyanobenzaldehyde, N-phenyl-(aza-15-crown-5), piperidine and phosphoryl chloride were purchased from Merck (Hohenbrunn, Germany). Benzaldehyde was purchased from Sigma-Aldrich (Steinheim, Germany) and 2,3-butanedione was purchased from Aldrich (Steinheim, Germany). Glacial acetic acid was obtained from Merck (Darmstadt, Germany). All solvents which are analytical and spectroscopic grade were obtained from Merck (Darmstadt, Germany), Panreac and Carlo Erba Reagents Group. Thin layer chromatography (TLC) was carried out with silica gel $60F_{254}$ from Merck (Darmstadt, Germany). Column chromatography purifications were carried out with 70-230 mesh silica gel (0.063-0.2 mm, Merck).

2.2 Synthesis

2.2.1 Synthesis of Derivatives 2

The general synthesis pathway of derivatives 2 is shown in Figure 2.1.

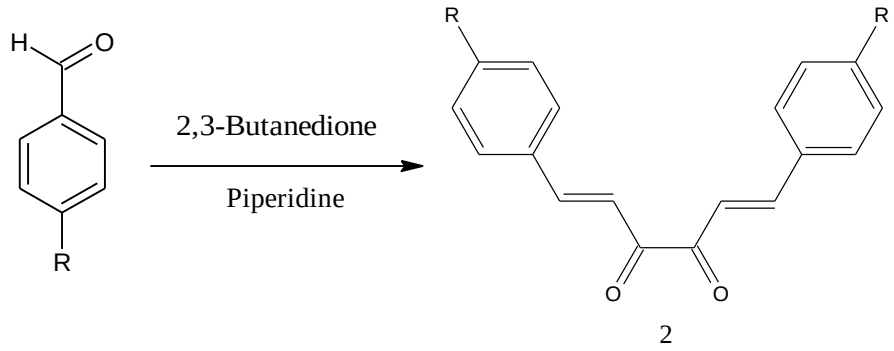

Figure 2.1 Synthesis of derivatives 2

Table 2.1 The derivatives 2

Compound	2a	2b	2c	2d
−R	−H	$-OCH_3$	$-NO_2$	−CN

Aromatic aldehyde (9 mmol) and methanol (20 mL) was added to a two-necked round bottom flask. Then, 2,3-butanedione (4.5 mmol) was added to the stirred mixture. Then glacial acetic acid (5 mmol) was added to the stirred reaction mixture. And as a last reagent, piperidine (5 mmol) was added to the reaction mixture drop by drop as catalyst. The reaction mixture was stirred under nitrogen atmosphere for 15 minutes at room temperature. The mixture was heated slowly and refluxed for 24 h under nitrogen atmosphere. After TLC monitoring showed consumption of aromatic aldehyde, the mixture was cooled to room temperature and methanol on a small scale was added to the reaction mixture. Then the mixture was waited until the precipitate was formed and then the precipitate was filtrated and washed with methanol for several times. The crude product was purified by column chromatography using ethyl acetate / n-hexane as eluent (Renouard et al., 2002).

2.2.1.1 The Derivative 2a

Figure 2.2 shows the molecular structure of 1,6-diphenylhexa-1,5-diene-3,4-dione (2a). For the synthesis of the compound 2a, the following amounts of five components were used.

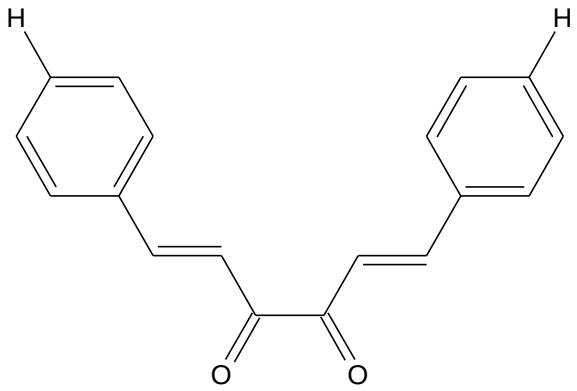

Figure 2.2 The derivative 2a

The amounts of five components for the compound 2a: 15.4 mL “150 mmol” benzaldehyde, 20 mL methanol, 6.8 mL “75 mmol” 2,3-butanedione, 4.77 mL “83.33 mmol” glacial acetic acid, 8.33 mL “83.33 mmol” piperidine.

2.2.1.2 The Derivative 2b

The molecular structure of 1,6-bis(4-methoxyphenyl)hexa-1,5-diene-3,4-dione (2b) is given in Figure 2.3. The compound 2b was synthesized with the following amounts of five components.

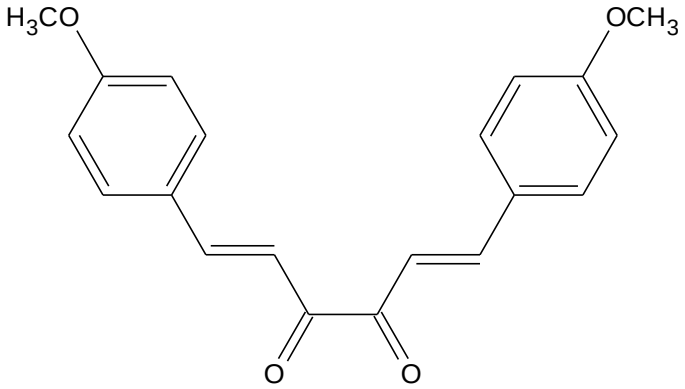

Figure 2.3 The derivative 2b

The amounts of five components for the compound 2b: 6.7 mL “54 mmol” 4-methoxybenzaldehyde, 20 mL methanol, 2.44 mL “27 mmol” 2,3-butanedione, 1.72 mL “30 mmol” glacial acetic acid, 3.0 mL “30 mmol” piperidine.

2.2.1.3 The Derivative 2c

The molecular structure of 1,6-bis(4-nitrophenyl)hexa-1,5-diene-3,4-dione (2c) is shown in Figure 2.4. For the synthesis of the compound 2c, the following amounts of five components were used.

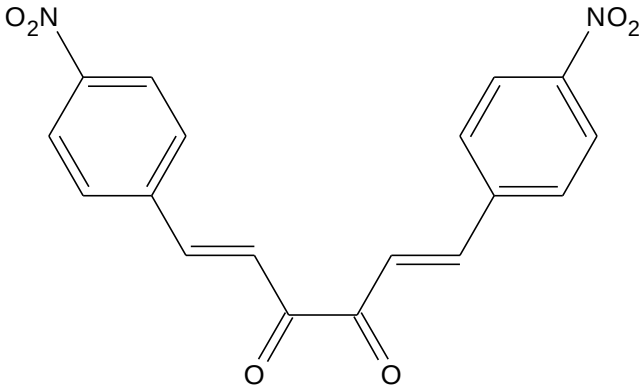

Figure 2.4 The derivative 2c

The amounts of five components for the compound 2c: 4 g “26.47 mmol” 4-nitrobenzaldehyde, 20 mL methanol, 1.2 mL “13.23 mmol” 2,3-butanedione, 0.84 mL “14.71 mmol” glacial acetic acid, 1.47 mL “14.71 mmol” piperidine.

2.2.1.4 The Derivative 2d

Figure 2.5 shows the molecular structure of 1,6-bis(4-cyanophenyl)hexa-1,5-diene-3,4-dione (2d). The compound 2d was synthesized with the following amounts of five components.

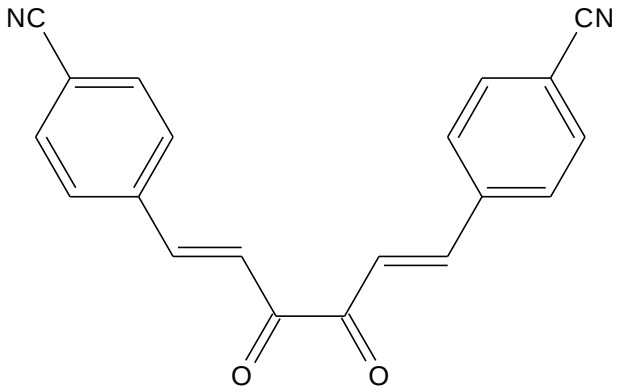

Figure 2.5 The derivative 2d

The amounts of five components for the compound 2d: 4 g “30.51 mmol” 4-cyanobenzaldehyde, 20 mL methanol, 1.38 mL “15.25 mmol” 2,3-butanedione, 0.97 mL “16.95 mmol” glacial acetic acid, 1.7 mL “16.95 mmol” piperidine.

2.2.2 Synthesis of 4-formylbenzo-aza-15-crown-5

The synthesis pathway of 4-formylbenzo-aza-15-crown-5 is shown in Figure 2.6.

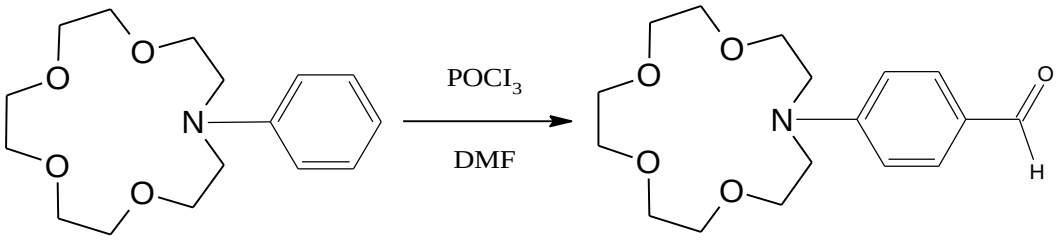

N-phenyl-aza-15-crown-5 4-formylbenzo-aza-15-crown-5

Figure 2.6 Synthesis of 4-formylbenzo-aza-15-crown-5

0.2 g (0.68 mmol) N-phenyl-aza-15-crown-5 and 0.62 mL (7.97 mmol) N,N-dimethylformamide (DMF) were added to a three-necked round bottom flask. The reaction mixture was stirred at room temperature for 30 min. The mixture was cooled to -10ºC under ice-salt bath. Then 0.063 mL (0.68 mmol) phosphoryl chloride ($POCl_3$) was added slowly to the stirred mixture drop by drop. The mixture was stirred for 30 min at -10ºC. Then the mixture was stirred for 1 h at room temperature. The reaction mixture was heated to 100ºC. After TLC monitoring showed consumption of N-phenyl-aza-15-crown-5, the mixture was cooled to room temperature and poured into pieces of ice and neutralized by 5 % of NaOH. Then the mixture was extracted with ethyl acetate, ethyl acetate was vaporized by evaporator. The crude product was purified by column chromatography using ethyl acetate / n-hexane as eluent (Mateeva, Deligeorgiev, Mitewa & Simova, 1992).

2.2.3 Synthesis of Derivatives 1

The general synthesis of derivatives 1 was performed as shown in Figure 2.7.

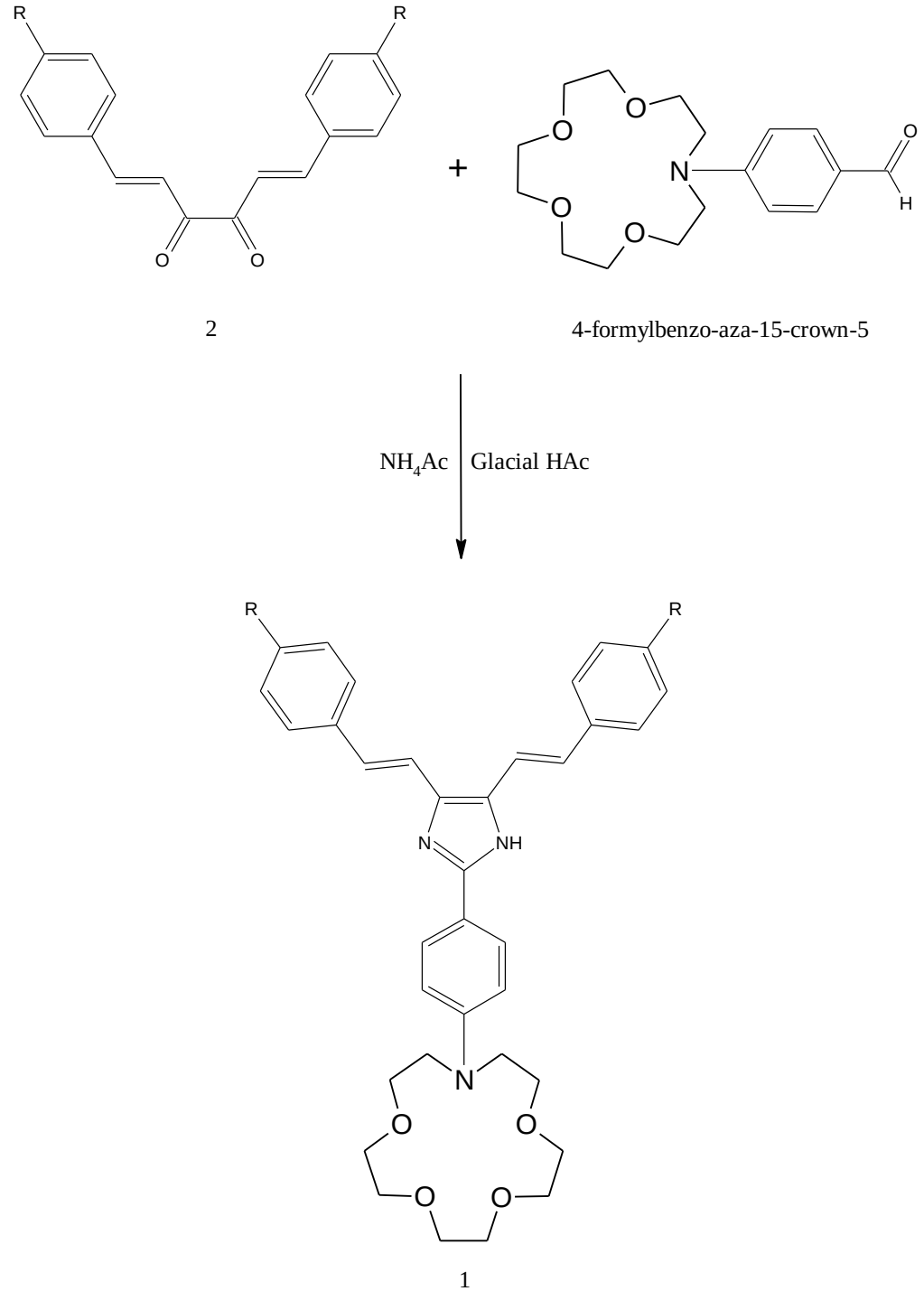

2 4-formylbenzo-aza-15-crown-5

1

Figure 2.7 Synthesis of derivatives 1

If derivative 2 is 1,6-diphenylhexa-1,5-diene-3,4-dione (2a), derivative 1 is 4,5-(2,2'-diphenyl)vinyl-{2-[(1,4,7,10-tetraoxa-13-azacyclopentadecyl)phenyl]}-1H-imidazole (1a). If derivative 2 is 1,6-bis(4-methoxyphenyl)hexa-1,5-diene-3,4-dione (2b), derivative 1 is 4,5-{[2,2'-bis(4-methoxyphenyl)vinyl]-[2-(1,4,7,10-tetraoxa-13-azacyclopentadecyl)phenyl]}-1H-imidazole (1b).

Glacial acetic acid (25 mL) and ammonium acetate (15 mmol) were added to a three-necked round bottom flask. The mixture was stirred until ammonium acetate was dissolved. 2 (1.5 mmol) was added to the stirred mixture and kept stirring at room temperature until 2 was dissolved. Then 4-formylbenzo-aza-15-crown-5 (1.5 mmol) was added in 1 h. The reaction mixture was stirred at room temperature under nitrogen atmosphere for 1 h. The mixture was heated to 90ºC and stirred at 90ºC under nitrogen atmosphere for 24 h and then cooled to room temperature. The cooled mixture poured into 100 mL of ice-water and neutralized by 5 % of ammonia. The formed precipitation was filtreted and washed with water several times. Then the crude product was redissolved in dimethyl sulfoxide (DMSO) and purified by column chromatography using (10:1) ethyl acetate / chloroform (100:1) DMSO. The obtained product was precipitated in chloroform / hexane and filtreted (Zhang et al., 2008).

2.2.3.1 The Derivative 1a

The molecular structure of 4,5-(2,2'-diphenyl)vinyl-{2-[(1,4,7,10-tetraoxa-13-azacyclopentadecyl)phenyl]}-1H-imidazole (1a) is given in Figure 2.8. The compound 1a was synthesized by the reaction of the following amount of four components.

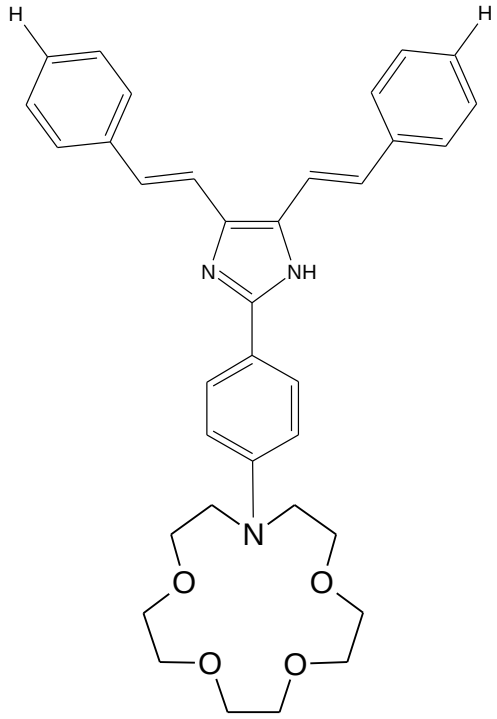

Figure 2.8 The derivative 1a

The amounts of four components for the compound 1a: 7.61 mL glacial acetic acid, 0.352 g “4.564 mmol” ammonium acetate, 0.1197 g “0.456 mmol” 2a, 0.1476 g “0.456 mmol” 4-formylbenzo-aza-15-crown-5.

2.2.3.2 The Derivative 1b

The molecular structure of 4,5-{[2,2'-bis(4-methoxyphenyl)vinyl]-[2-(1,4,7,10-tetraoxa-13-azacyclopentadecyl)phenyl]}-1H-imidazole (1b) is given in Figure 2.9. The compound 1b was obtained by the reaction of the following amount of four components.

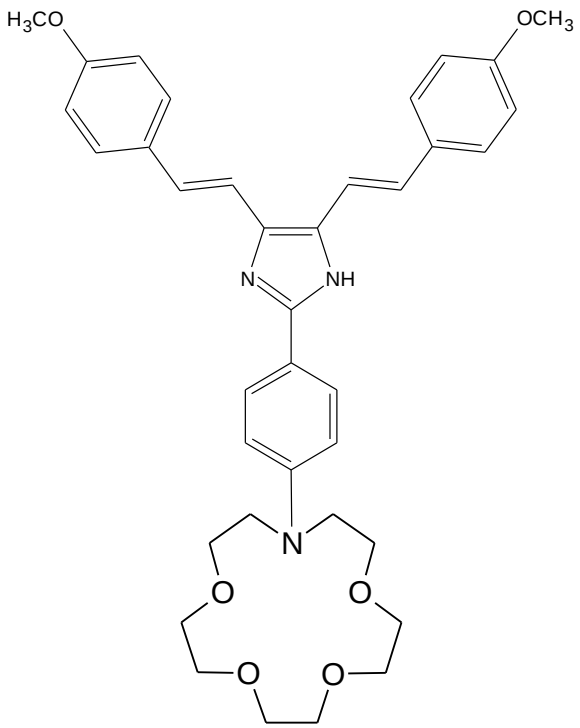

Figure 2.9 The derivative 1b

The amounts of four components for the compound 1b: 7.73 mL glacial acetic acid, 0.358 g “4.638 mmol” ammonium acetate, 0.1495 g “0.464 mmol” 2b, 0.150 g “0.464 mmol” 4-formylbenzo-aza-15-crown-5.

2.3 Structural and Spectral Analysis

The structures of synthesized compounds were confirmed by FT-IR and ^{1}H-NMR. ^{1}H-NMR spectra were recorded on a Varian Mercury AS-400 (400 MHz) spectrometer. Fourier transform infrared spectra were measured on a Perkin Elmer FTIR spectrophotometer (spectrum BX-II) as KBr discs. The UV-visible absorption spectra were obtained with Shimadzu UV-1800 spectrophotometer. The emission spectra were obtained on Varian-Cary Eclipse fluorescence spectrophotometer. All melting points were obtained by an electrothermal digital melting points apparatus (Southend, UK).

CHAPTER THREE
RESULTS AND DISCUSSION

3.1 Structural Analysis of The Synthesized Derivatives

3.1.1 Structural Analysis of Derivatives 2

3.1.1.1 Structural Analysis of 2a

The compound 2a, 1,6-diphenylhexa-1,5-diene-3,4-dione (Figure 3.1) was obtained as brown solid with yield of 17 % and its melting point was determined as 179ºC (Table 3.1). The characteristic vibration frequencies of 2a were shown in Table 3.2.

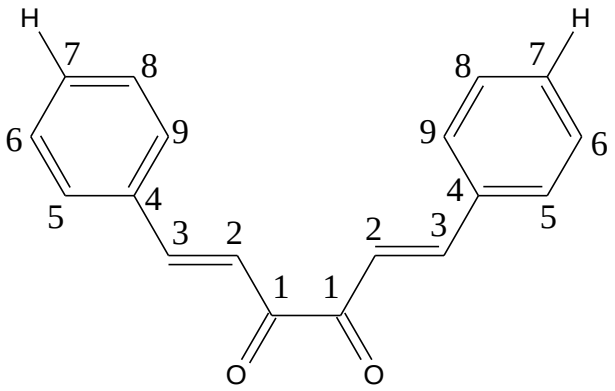

Figure 3.1 The structure of 2a

Table 3.1 Molecular weight (M.W.), color, melting point (M.P.) and yield of 2a

M.W. (g/mol)	Color	M.P. (ºC)	Yield (%)
262.30256	brown	179	17

Table 3.2 FT-IR data of 2a

ν (=C−H)$_{str}$ (cm^{-1})	ν (C=O)$_{str}$ (cm^{-1})	ν (C=C)$_{str}$ (cm^{-1})	ν (C−O)$_{str}$ (cm^{-1})
3058, 3026	1694	1601	1271

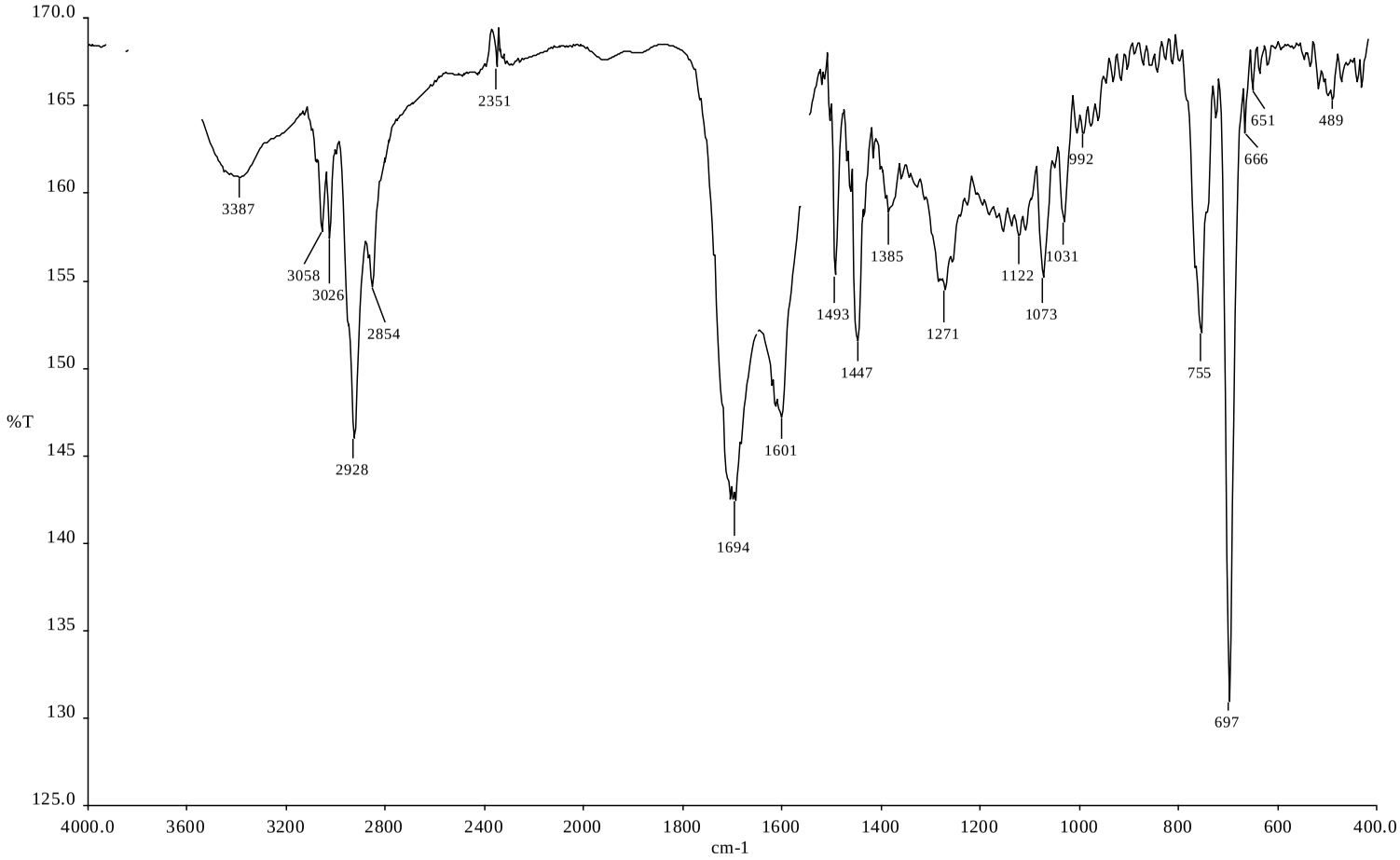

Figure 3.2 FT-IR spectrum of 2a in KBr

3.1.1.2 Structural Analysis of 2b

The compound 2b, 1,6-bis(4-methoxyphenyl)hexa-1,5-diene-3,4-dione (Figure 3.3) was synthesized as dark brown solid with yield of 28 % and its melting point was determined as 190°C (Table 3.3). The characteristic vibration frequencies of 2b are given in Table 3.4.

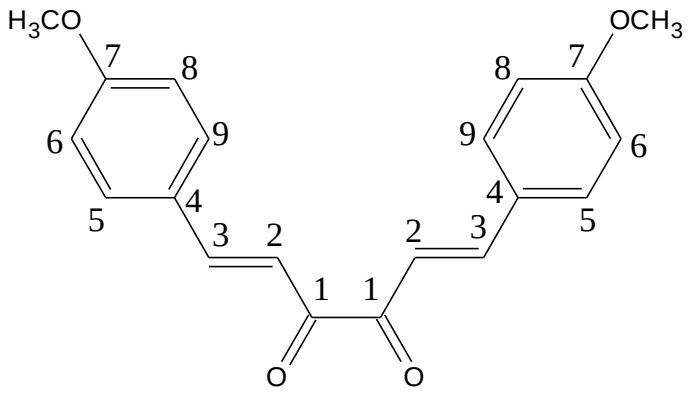

Figure 3.3 The structure of 2b

Table 3.3 Molecular weight (M.W.), color, melting point (M.P.) and yield of 2b

M.W. (g/mol)	Color	M.P. (ºC)	Yield (%)
322.35452	dark brown	190	28

Table 3.4 FT-IR data of 2b

ν (=C−H)$_{str}$ (cm^{-1})	ν (C=O)$_{str}$ (cm^{-1})	ν (C=C)$_{str}$ (cm^{-1})	ν (C−O)$_{str}$ (cm^{-1})
3031	1684	1599	1250

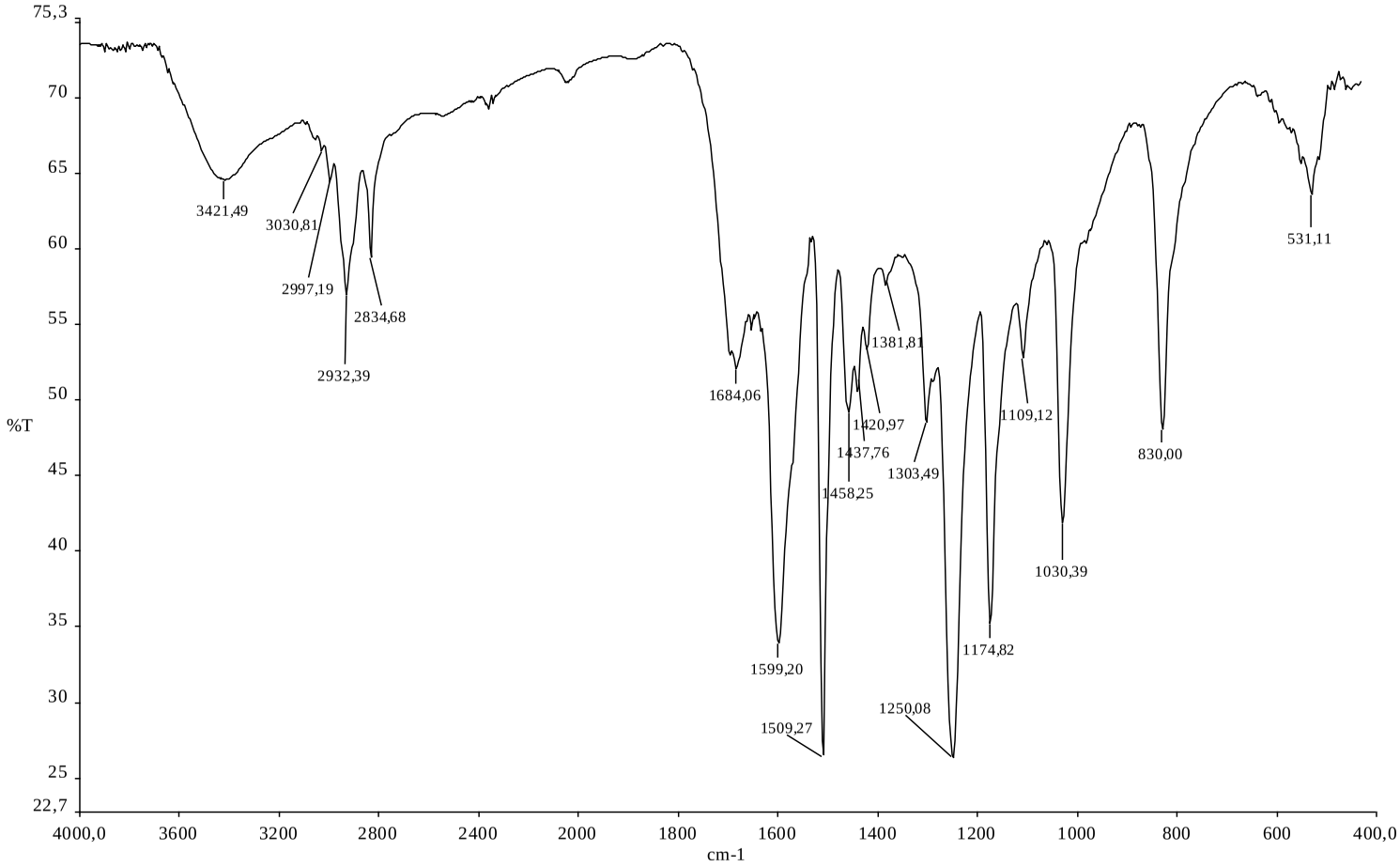

Figure 3.4 FT-IR spectrum of 2b in KBr

3.1.1.3 Structural Analysis of 2c

The compound 2c, 1,6-bis(4-nitrophenyl)hexa-1,5-diene-3,4-dione (Figure 3.5) was synthesized as dark orange solid with yield of 53 % and its melting point was observed as 108°C (Table 3.5). 2c exhibited the characteristic vibration frequencies as given in Table 3.6.

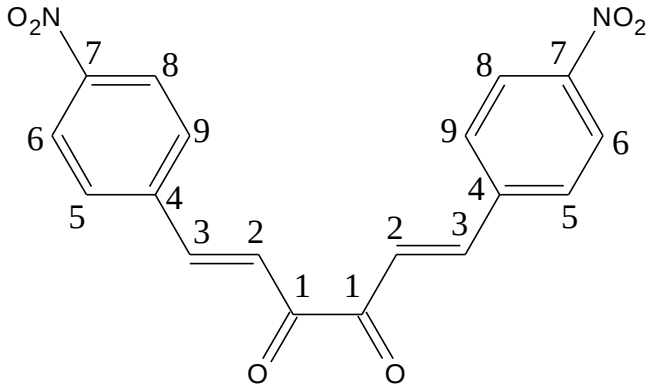

Figure 3.5 The structure of 2c

Table 3.5 Molecular weight (M.W.), color, melting point (M.P.) and yield of 2c

M.W. (g/mol)	Color	M.P. (ºC)	Yield (%)
352.29878	dark orange	108	53

Table 3.6 FT-IR data of 2c

ν $(=C-H)_{str}$ (cm^{-1})	ν $(C=O)_{str}$ (cm^{-1})	ν $(C=C)_{str}$ (cm^{-1})	ν $(NO_2)_{str}$ (cm^{-1})	ν $(C-O)_{str}$ (cm^{-1})
3074	1704	1595	1518 (asymmetric str.) 1345 (symmetric str.)	1180

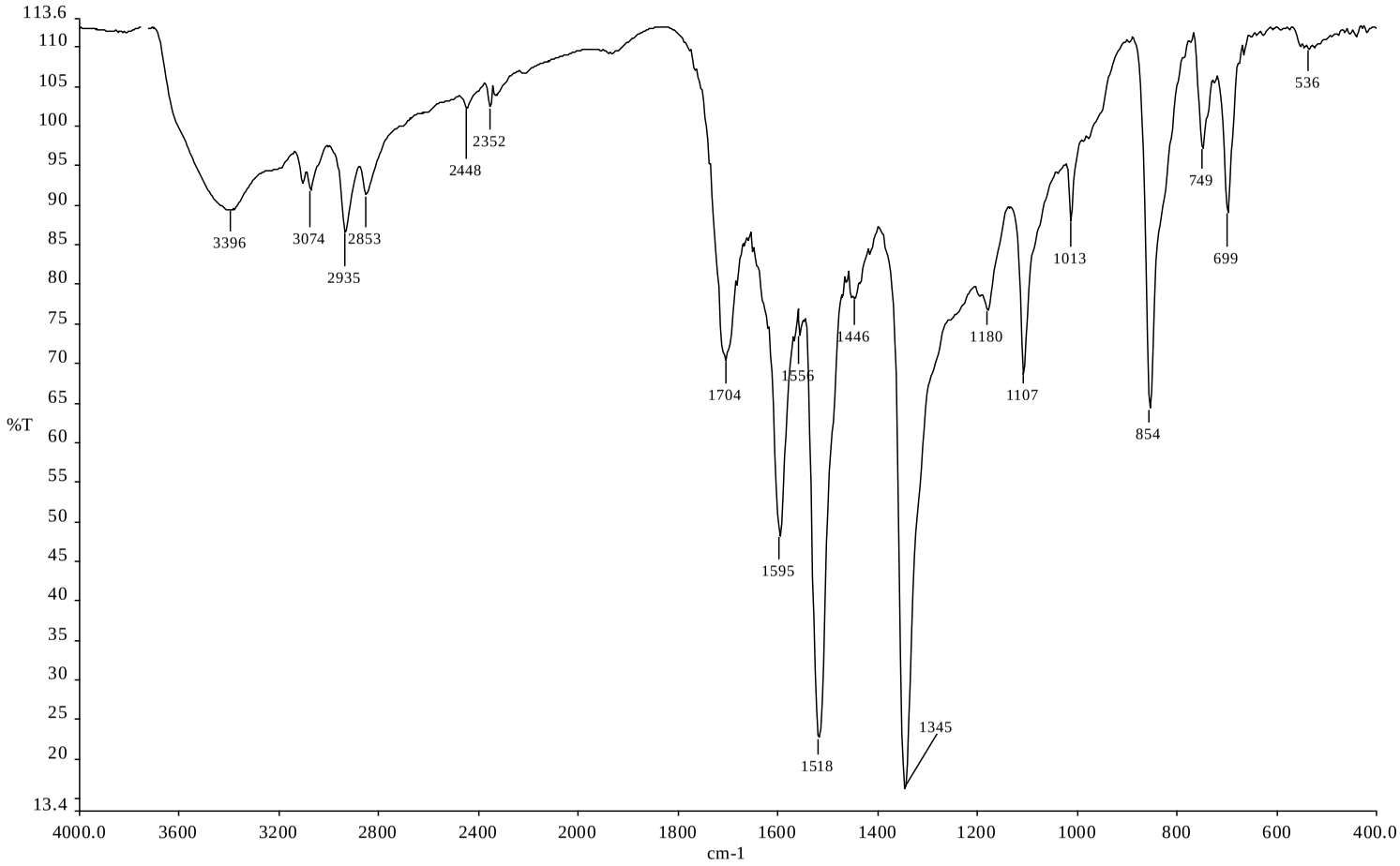

Figure 3.6 FT-IR spectrum of 2c in KBr

3.1.1.4 Structural Analysis of 2d

The compound 2d, 1,6-bis(4-cyanophenyl)hexa-1,5-diene-3,4-dione (Figure 3.7) was synthesized as dark orange solid with yield of 33 % and its melting point was determined as 286°C (Table 3.7). 2d showed the characteristic vibration frequencies as given in Table 3.8.

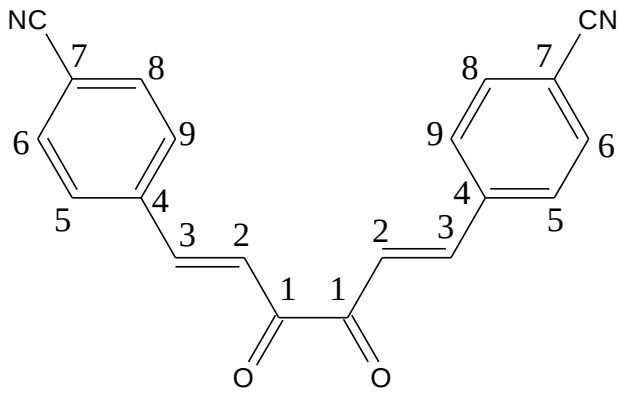

Figure 3.7 The structure of 2d

Table 3.7 Molecular weight (M.W.), color, melting point (M.P.) and yield of 2d

M.W. (g/mol)	Color	M.P. (ºC)	Yield (%)
312.32148	dark orange	286	33

Table 3.8 FT-IR data of 2d

ν (=C−H)$_{str}$ (cm^{-1})	ν (CN)$_{str}$ (cm^{-1})	ν (C=O)$_{str}$ (cm^{-1})	ν (C=C)$_{str}$ (cm^{-1})	ν (C−O)$_{str}$ (cm^{-1})
3063	2227	1700	1604	1275

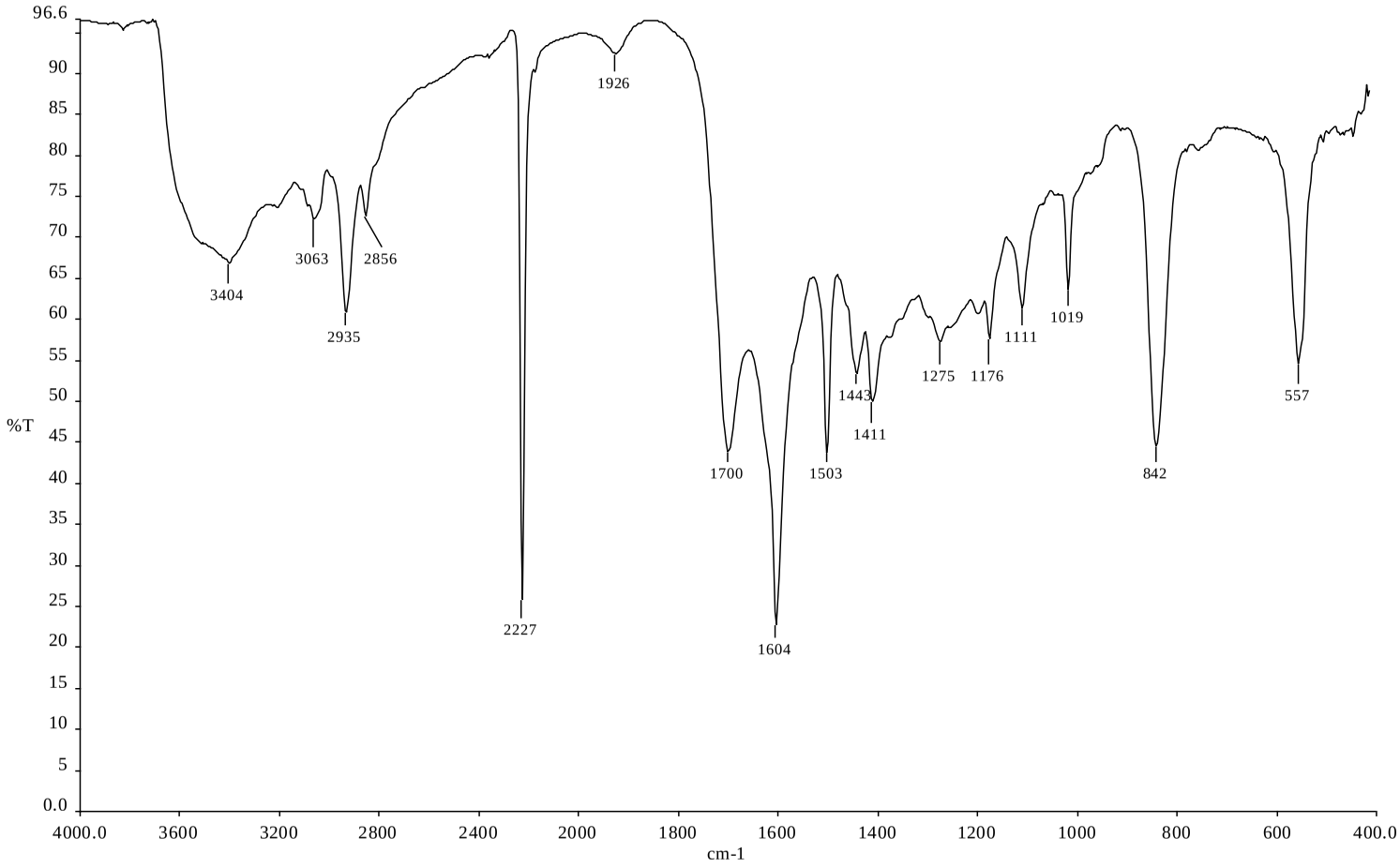

Figure 3.8 FT-IR spectrum of 2d in KBr

3.1.2 Structural Analysis of 4-formylbenzo-aza-15-crown-5

4-formylbenzo-aza-15-crown-5 (Figure 3.9) was synthesized as orange solid with yield of 67 % and its melting point was determined as 87-88°C (Table 3.9). The characteristic vibration frequencies for 4-formylbenzo-aza-15-crown-5 are given in Table 3.10.

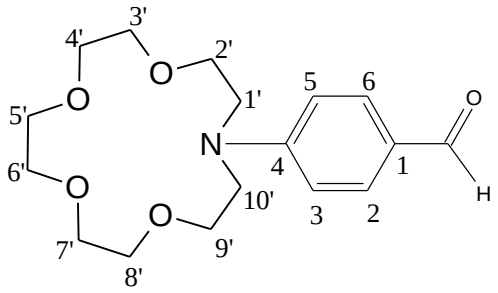

Figure 3.9 The structure of 4-formylbenzo-aza-15-crown-5

Table 3.9 Molecular weight (M.W.), color, melting point (M.P.) and yield of 4-formylbenzo-aza-15-crown-5

M.W. (g/mol)	Color	M.P. (ºC)	Yield (%)
323.3841	orange	87-88	67

Table 3.10 FT-IR data of 4-formylbenzo-aza-15-crown-5

ν $(O=C-H)_{str}$ (cm^{-1})	ν $(C=O)_{str}$ (cm^{-1})	ν $(=C-N)_{str}$ (cm^{-1})	ν $(C-O)_{str}$ (cm^{-1})
2728	1666	1600	1125

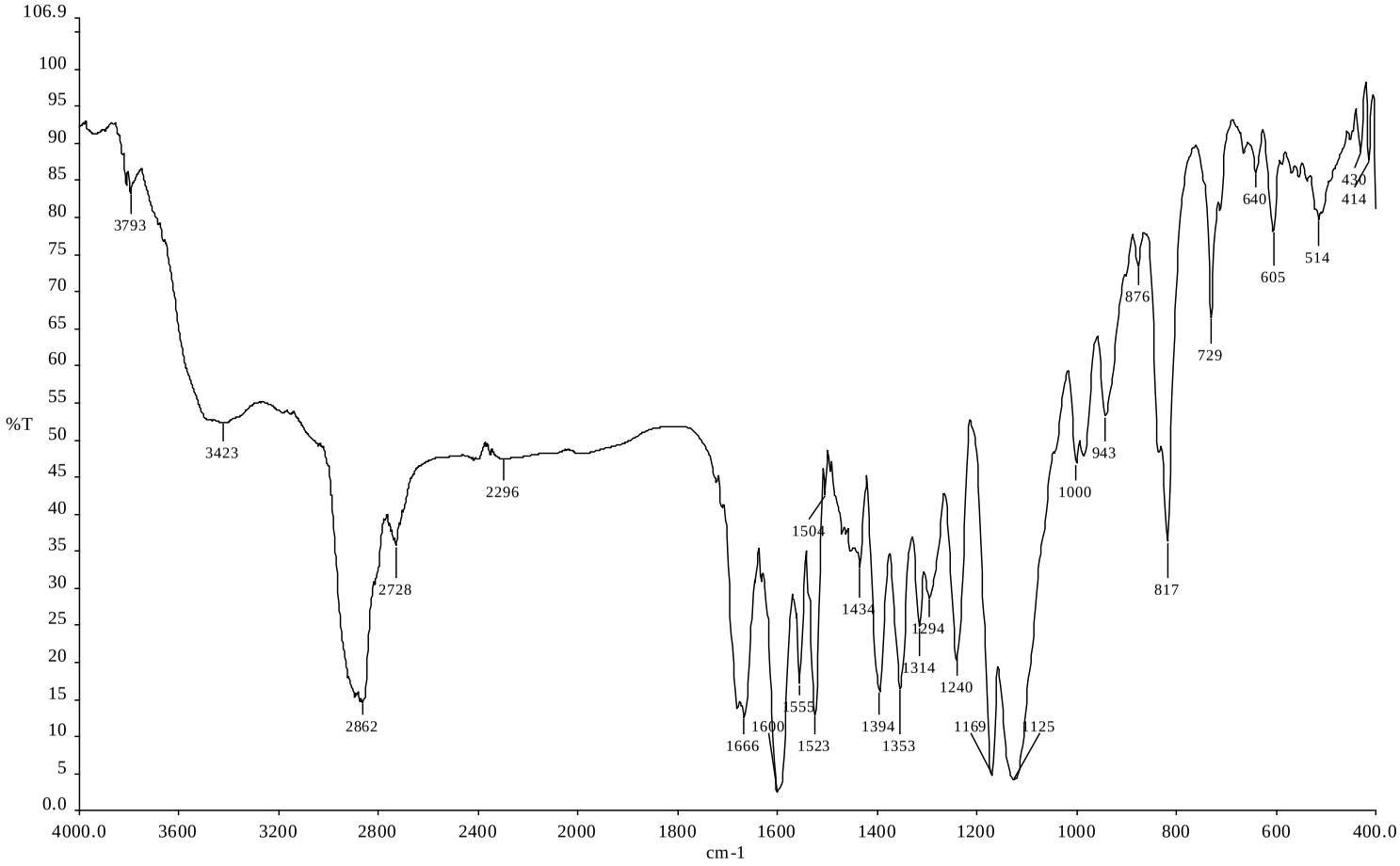

Figure 3.10 FT-IR spectrum of 4-formylbenzo-aza-15-crown-5 in KBr

The ^{1}H-NMR data for 4-formylbenzo-aza-15-crown-5 are given in Table 3.11. The singlet at 9.7 ppm reveals the formation of aldehyde.

Table 3.11 ^{1}H-NMR data of 4-formylbenzo-aza-15-crown-5

δ (Aldehyde proton) (ppm)	δ (Phenyl ring protons) (ppm)	δ (Crown ether protons) (ppm)
9.70 (s, 1H)	(7.67-7.69, d, 2H) [H_2, H_6] (6.67-6.69, d, 2H) [H_3, H_5]	(3.75-3.78, t, 4H) [H_1',H_{10}'] (3.64-3.67, t, 4H) [H_2', H_9'] (3.60, d, 2H) [H_5', H_6'] (3.62, s, 8H) [H_3', H_4', H_7', H_8']

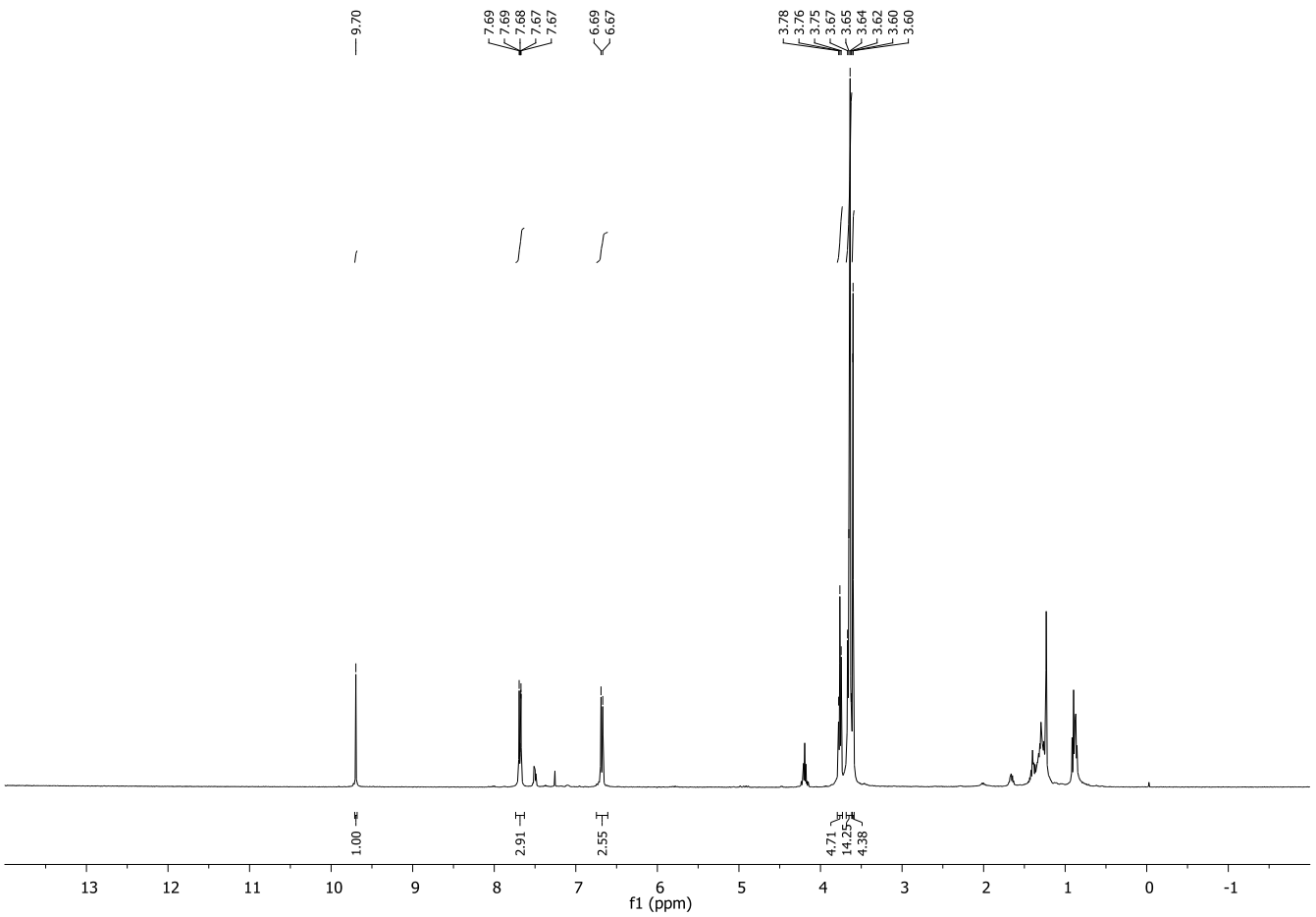

Figure 3.11 ^{1}H-NMR spectrum of 4-formylbenzo-aza-15-crown-5 in $CDCl_3$

3.1.3 Structural Analysis of Derivatives 1

3.1.3.1 Structural Analysis of 1a

The compound 1a, 4,5-(2,2'-diphenyl)vinyl-{2-[(1,4,7,10-tetraoxa-13-azacyclopentadecyl)phenyl]}-1H-imidazole (Figure 3.12) was synthesized as dark brown solid with yield of 13 % and its melting point was determined as 237°C (Table 3.12).

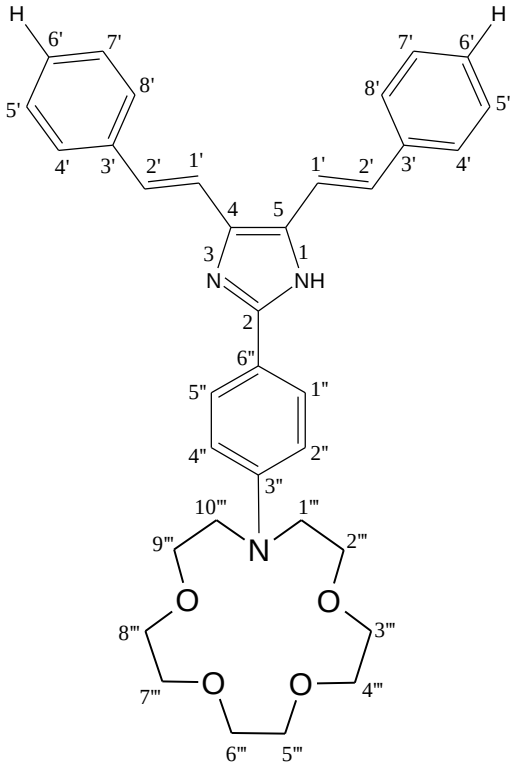

Figure 3.12 The structure of 1a

Table 3.12 Molecular weight (M.W.), color, melting point (M.P.) and yield of 1a

M.W. (g/mol)	Color	M.P. (ºC)	Yield (%)
565.70186	brown	237	13

The characteristic vibration frequencies of the compound 1a are given in Table 3.13. The vibration frequency of −N−H streching at 3422 cm^{-1} confirms the formation of 1a.

Table 3.13 FT-IR data of 1a

ν (−N−H)$_{str}$ (cm^{-1})	ν (−C=N)$_{str}$ (cm^{-1})	ν (−C=C)$_{str}$ (cm^{-1})	ν (−C−N)$_{str}$ (cm^{-1})	ν (−C−O)$_{str}$ (cm^{-1})
3422	1606	1519	1246	1118

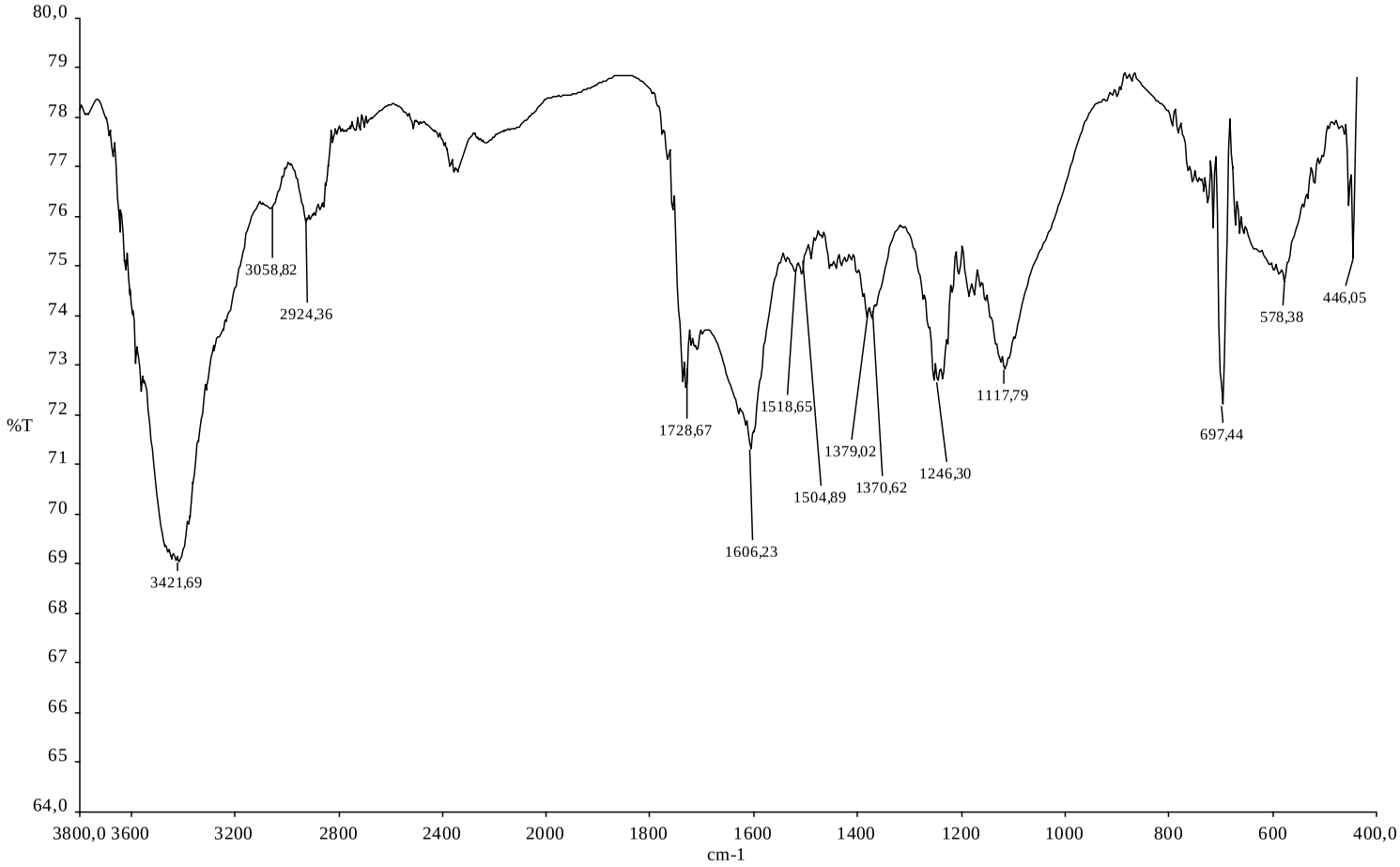

Figure 3.13 FT-IR spectrum of 1a in KBr

The ^{1}H-NMR data for the compound 1a are given in Table 3.14. The singlet at 12.72 ppm indicates −N−H hydrogen, confirming the formation of 1a.

Table 3.14 ^{1}H-NMR data of 1a

δ (−N−H) (ppm)	δ (Phenyl and vinyl protons) (ppm)	δ (Crown ether protons) (ppm)
12.72 (s, 1H)	(7.72 - 6.38, m, 18H) [H_1', H_2', H_4', H_5', H_6', H_7', H_8'] [H_1'', H_2'', H_4'', H_5'']	(3.82 - 3.35, m, 20H) [H_1''', H_2''', H_3''', H_4''', H_5''', H_6''', H_7''', H_8''', H_9''', H_{10}''']

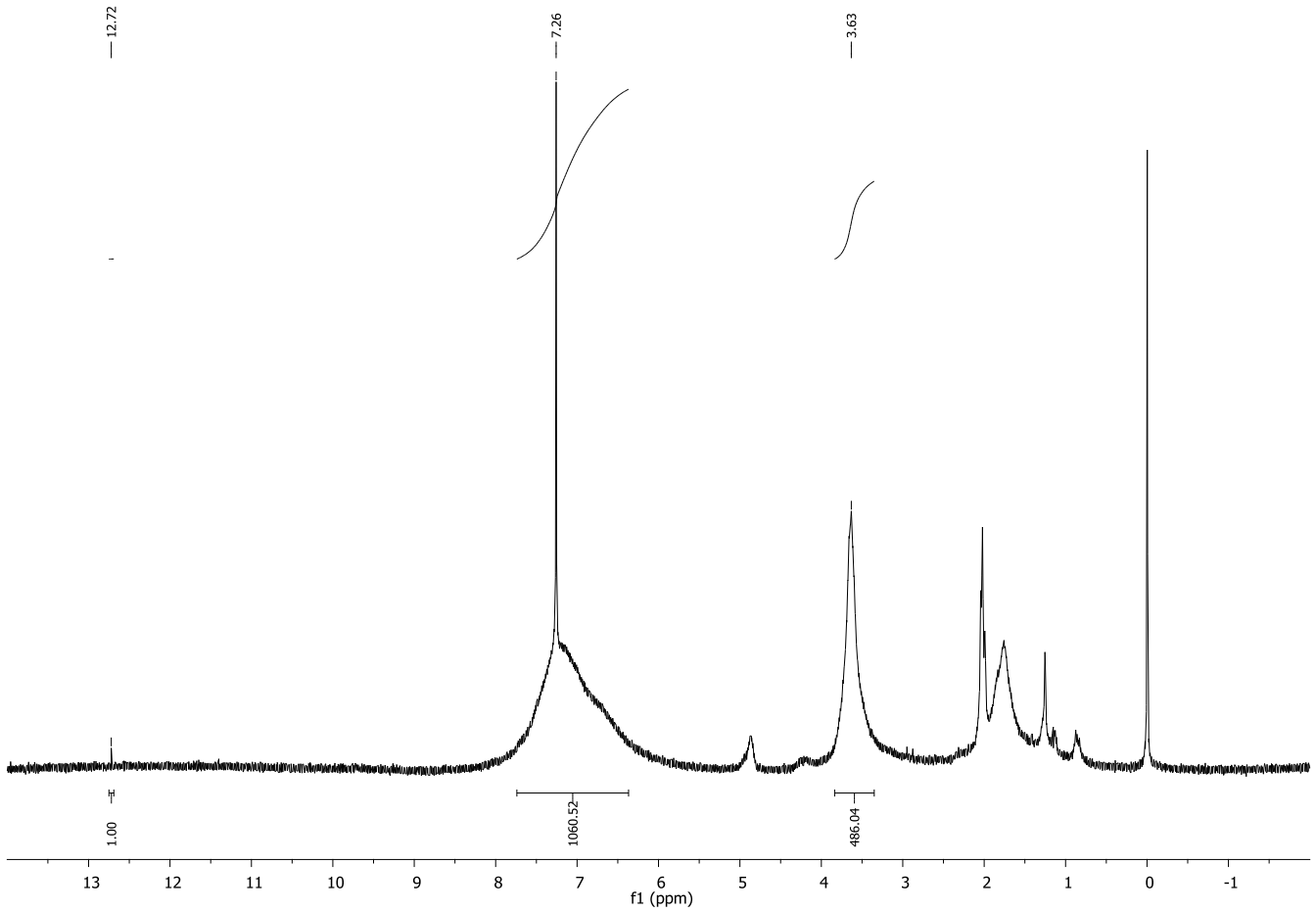

Figure 3.14 ^{1}H-NMR spectrum of 1a in $CDCl_3$

3.1.3.2 Structural Analysis of 1b

The compound 1b, 4,5-{[2,2'-bis(4-methoxyphenyl)vinyl]-[2-(1,4,7,10-tetraoxa-13-azacyclopentadecyl)phenyl]}-1H-imidazole (Figure 3.15) was synthesized as dark brown solid with yield of 9 % and its melting point was determined as 146°C (Table 3.15).

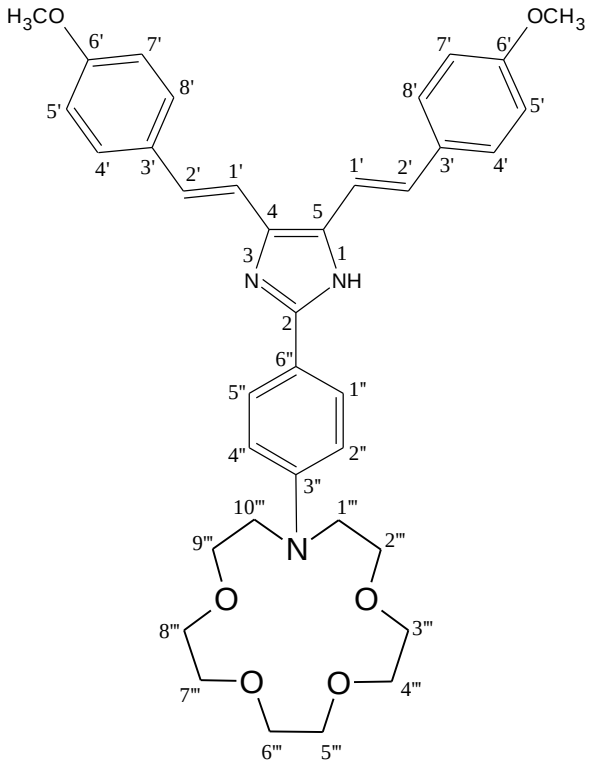

Figure 3.15 The structure of 1b

Table 3.15 Molecular weight (M.W.), color, melting point (M.P.) and yield of 1b

M.W. (g/mol)	Color	M.P. (ºC)	Yield (%)
625.75382	brown	146	9

The characteristic vibration frequencies of the compound 1b are given in Table 3.16. The vibration frequency of −N−H streching at 3438 cm^{-1} confirms the formation of 1b.

Table 3.16 FT-IR data of 1b

ν (−N−H)$_{str}$ (cm^{-1})	ν (−C=N)$_{str}$ (cm^{-1})	ν (−C=C)$_{str}$ (cm^{-1})	ν (−C−N)$_{str}$ (cm^{-1})	ν (−C−O)$_{str}$ (cm^{-1})
3438	1607	1511	1250	1177

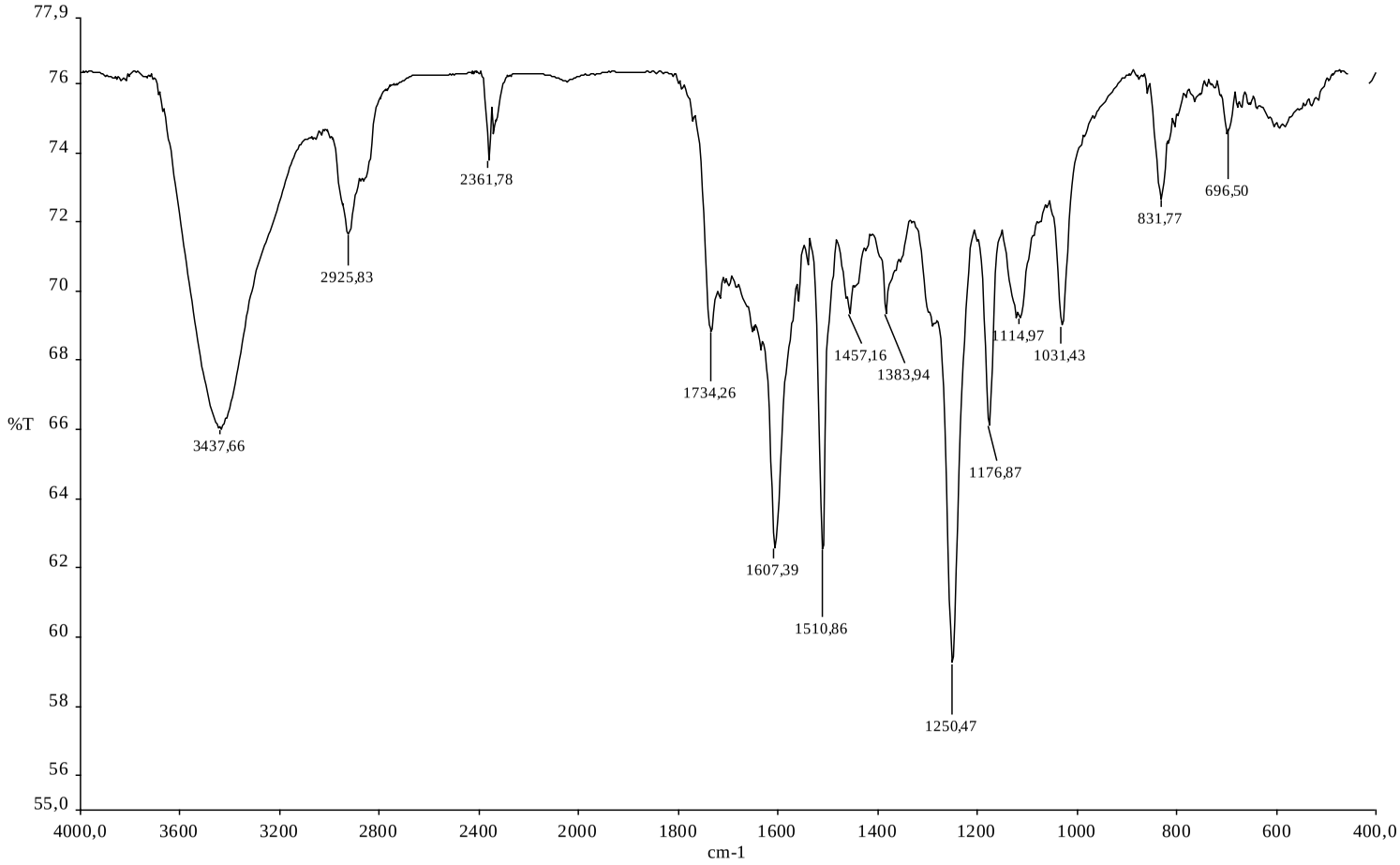

Figure 3.16 FT-IR spectrum of 1b in KBr

The ^{1}H-NMR data for the compound 1b are given in Table 3.17. The singlet at 12.73 ppm indicates −N−H hydrogen, confirming the formation of 1b.

Table 3.17 ^{1}H-NMR data of 1b

δ (−N−H) (ppm)	δ (Phenyl and vinyl protons) (ppm)	δ (Crown ether protons), δ (−OCH_3) (ppm)
12.73 (s, 1H)	(7.49 - 6.28, m, 16H) [H_1', H_2', H_4', H_5', H_7', H_8'] [H_1'', H_2'', H_4'', H_5'']	(3.98 - 3.13, m, 26H) [H_1''', H_2''', H_3''', H_4''', H_5''', H_6''', H_7''', H_8''', H_9''', H_{10}''']

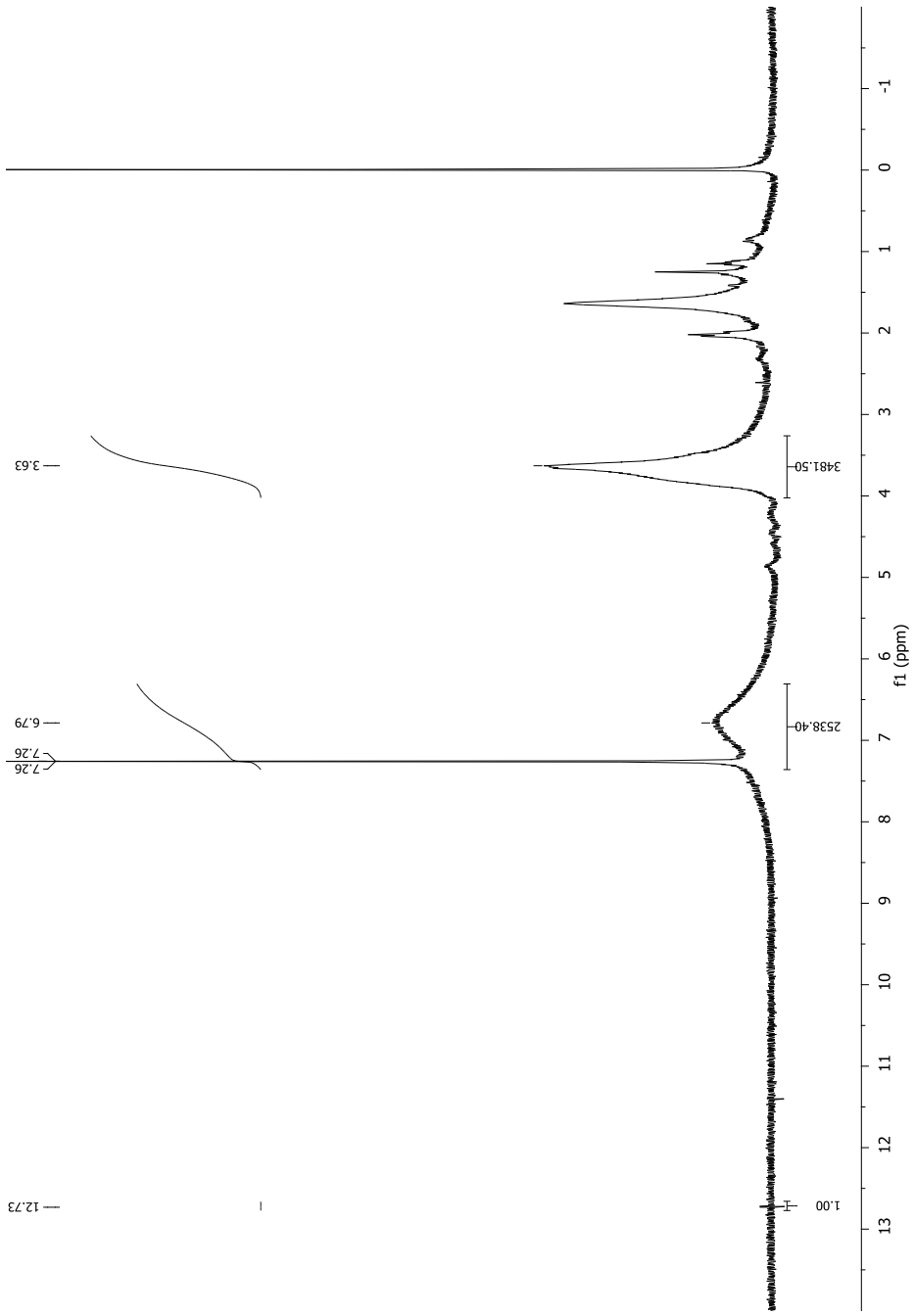

Figure 3.17 ^{1}H-NMR spectrum of 1b in $CDCl_3$

3.2 Absorption and Fluorescence Characteristics of Derivatives 1

3.2.1 Absorption and Emission Parameters of 1a and 1b

The absorption and emission spectra of compounds 1a and 1b were recorded in six solvents which are toluene, dichloromethane, tetrahydrofuran, ethyl acetate, acetonitrile and N,N-dimethylformamide. The absorption and emission spectra were obtained by using an UV-vis spectrophotometer and a fluorescence spectrophotometer in the range of 400 – 800 nm, respectively. The absorption and emission spectra of derivatives 1a and 1b are shown in Figure 3.18 – 3.29.

The photophysical properties such as maximum absorption wavelengths (λ_{max}^{abs}, nm), maximum emission wavelengths (λ_{max}^{emis}, nm), Stokes' shifts ($\Delta\lambda$, nm), singlet energies (E_s, kcal mol^{-1}), fluorescence quantum yields ($\O_F$) and photostabilities of derivatives 1a and 1b were investigated by measuring absorption and emission spectra in a series of solvents of varying polarity toluene (TOL), dichloromethane (DCM), tetrahydrofuran (THF), ethyl acetate (EA), acetonitrile (ACN) and N,N-dimethylformamide (DMF) at the concentration of 5 x 10^{-6} M. Both of these derivatives showed two maximum absorption wavelength values in the UV-vis region and three intense maximum emission wavelength values in the visible region. Absorption and fluorescence emission data of 1a and 1b are given in Table 3.18 and Table 3.19, respectively.

The quantum yield values of the synthesized compounds 1a and 1b were also investigated. The fluorescence quantum yields were determined by using quinine sulphate in 0.1 M sulphuric acid (H_2SO_4) as a reference in six solvents; toluene, dichloromethane, tetrahydrofuran, ethyl acetate, acetonitrile and N,N-dimethyformamide. The emission maximum wavelength and quantum yield value of quinine sulphate in 0.1 M sulphuric acid are 574 nm and 0.54, respectively.

The photostabilities of derivatives 1a and 1b in toluene, dichloromethane, tetrahydrofuran, ethyl acetate, acetonitrile, N,N-dimethylformamide were determined

by using a steady-state spectrofluorometer in time based mode. The compounds were excited at their absorption maxima and the data were acquired at their maximum emission wavelengths. The data collected after 1 h of monitoring shown in Figure 3.30 – 3.41 reveals the excellent photostability of 1a and 1b in all the solvents tested.

Table 3.18 Absorption and fluorescence emission data of 1a

Compound	Solvent	λ_{max1}^{abs}	λ_{max2}^{abs}	ε_{max1}	ε_{max2}	λ_{max1}^{emis}	λ_{max2}^{emis}	λ_{max3}^{emis}	$\Delta\lambda$	E_{s1}	E_{s2}	E_{s3}	$Ø_F$
1a	TOL	284	326	31660	20000	422	530	644	96	67.6	53.8	44.3	0.1466
	DCM	262	343	49300	29040	425	532	677	82	67.1	53.6	42.1	0.1684
	THF	269	325	59280	19200	412	512	642	87	69.2	55.7	44.5	0.1615
	EA	262	324	51740	20800	423	548	638	99	67.4	52.1	44.7	0.1730
	ACN	269	321	49260	18180	423	471	633	102	67.4	60.6	45.1	0.2445
	DMF	269	329	40540	23060	422	485	649	93	67.6	58.8	44.0	0.1415

Table 3.19 Absorption and fluorescence emission data of 1b

Compound	Solvent	λ_{max1}^{abs}	λ_{max2}^{abs}	ε_{max1}	ε_{max2}	λ_{max1}^{emis}	λ_{max2}^{emis}	λ_{max3}^{emis}	$\Delta\lambda$	E_{S1}	E_{s2}	E_{s3}	$Ø_F$
1b	TOL	285	331	77760	22480	425	499	653	94	67.1	57.1	43.7	0.3107
	DCM	269	323	38600	23480	434	502	638	111	65.7	56.8	44.7	0.2488
	THF	269	333	62640	24600	428	490	657	95	66.7	58.2	43.4	0.2632
	EA	269	328	52540	20940	430	494	648	102	66.4	57.8	44.1	0.2686
	ACN	279	327	40320	25060	418	471	648	91	68.3	60.6	44.0	0.1628
	DMF	-	322	-	21780	428	479	635	106	66.7	59.6	44.9	0.2322

Absorption spectra of derivatives 1 were recorded in six solvents at the concentration of 5 x 10^{-6} M and they are shown in Figure 3.18 – 3.23.

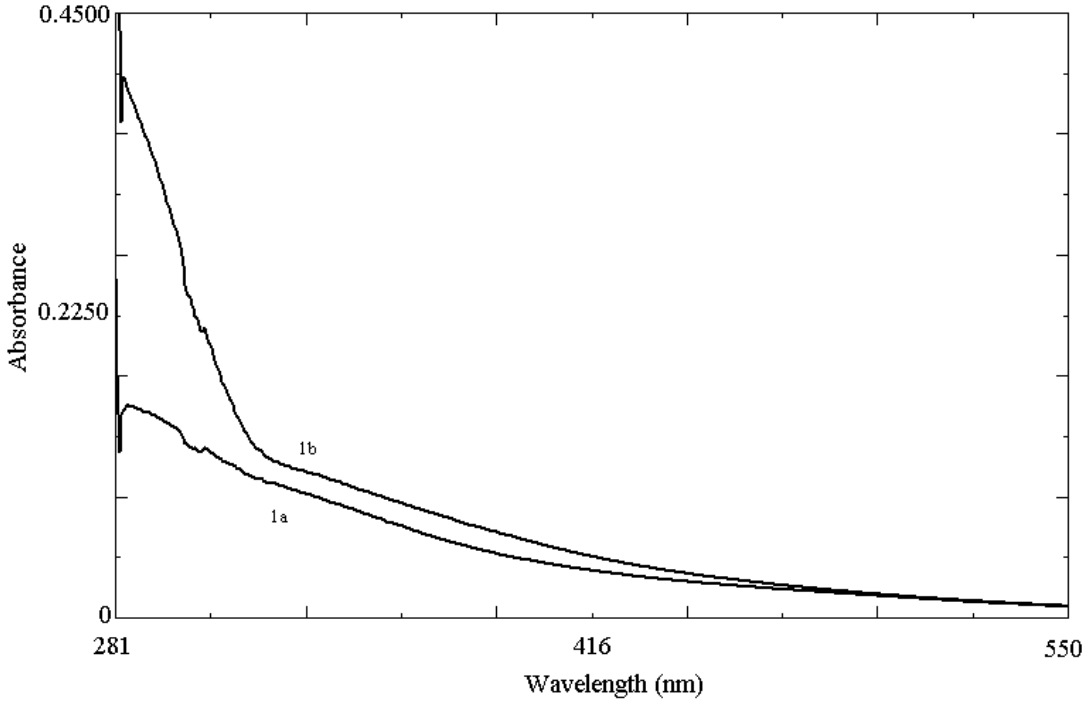

Figure 3.18 Absorption spectra of 1a and 1b in toluene

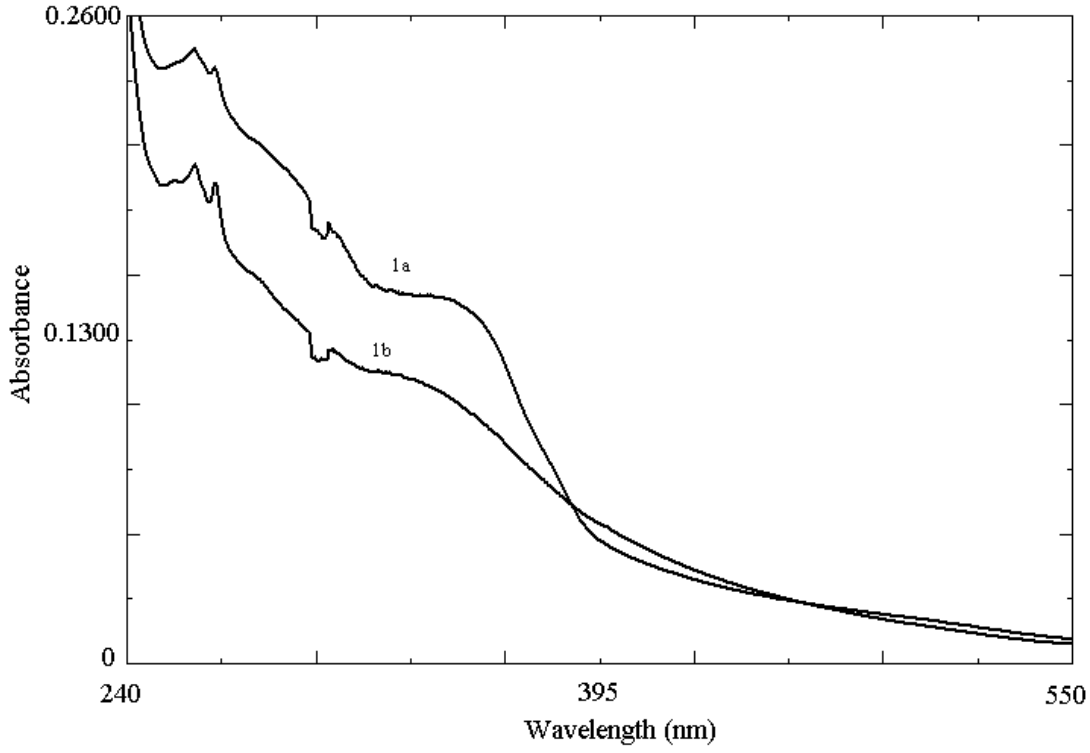

Figure 3.19 Absorption spectra of 1a and 1b in dichloromethane

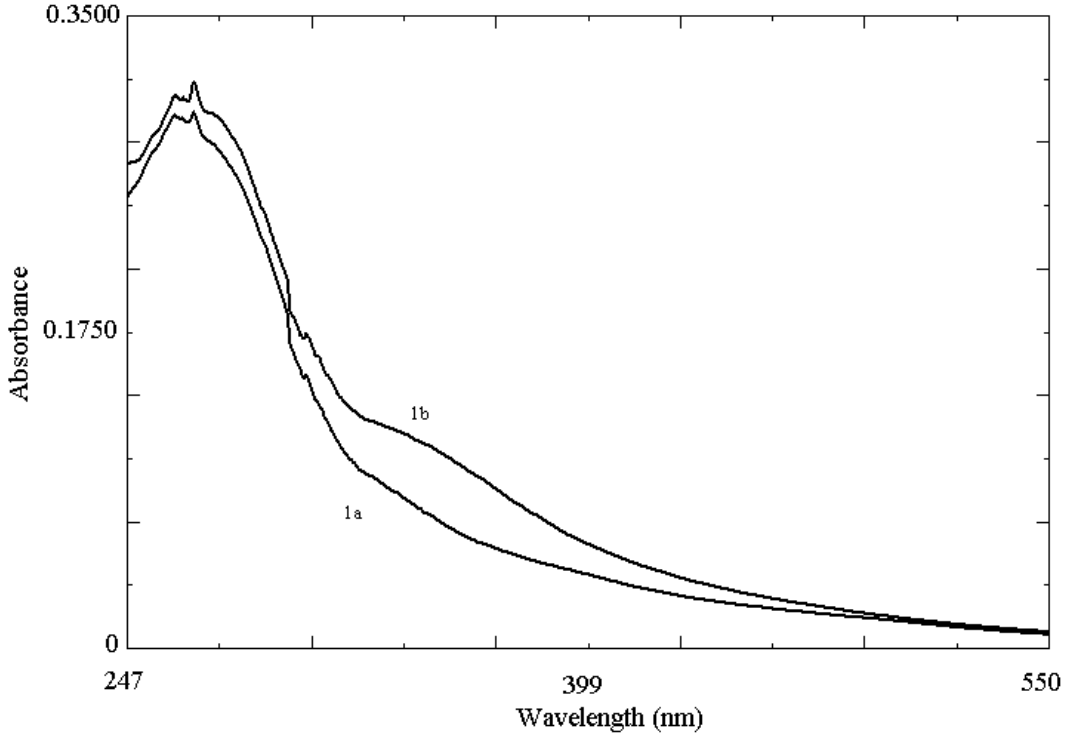

Figure 3.20 Absorption spectra of 1a and 1b in tetrahydrofuran

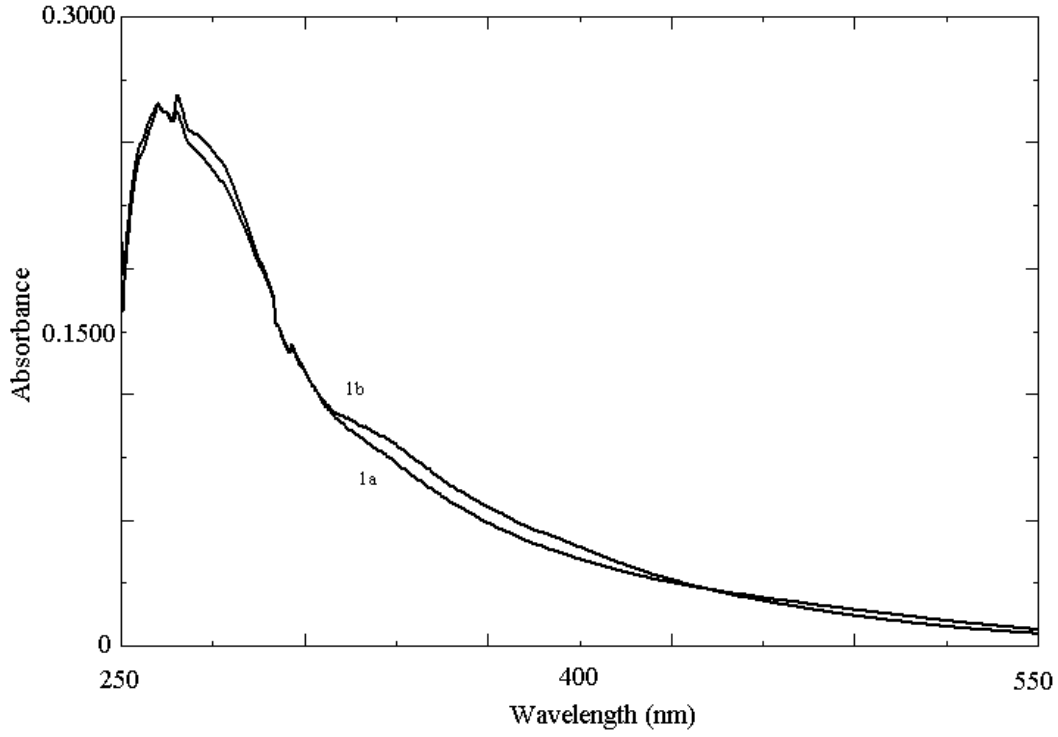

Figure 3.21 Absorption spectra of 1a and 1b in ethyl acetate

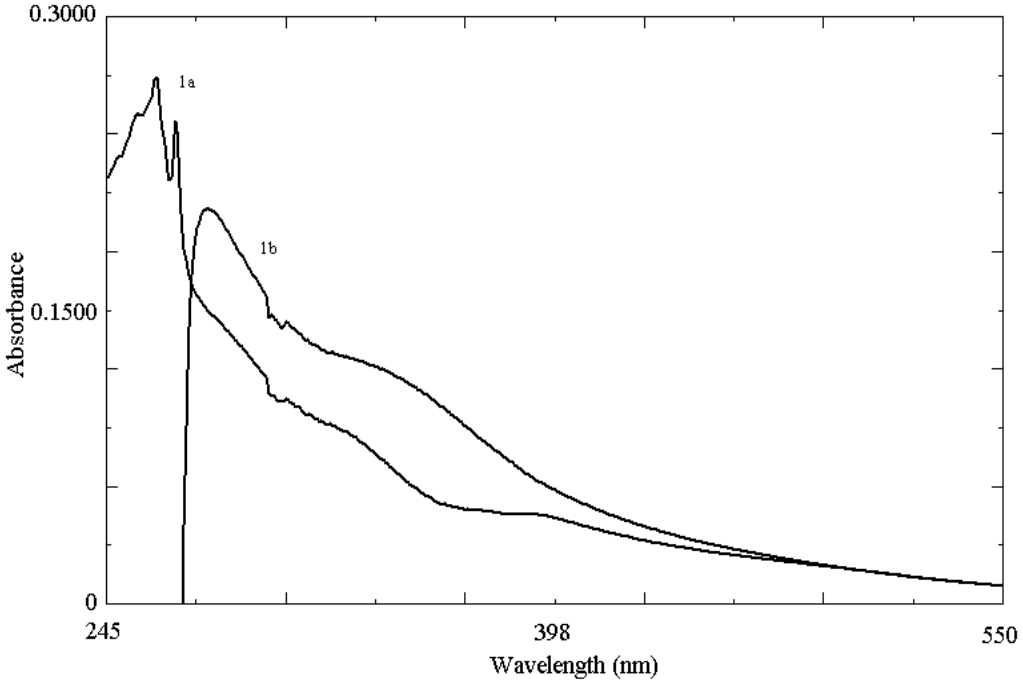

Figure 3.22 Absorption spectra of 1a and 1b in acetonitrile

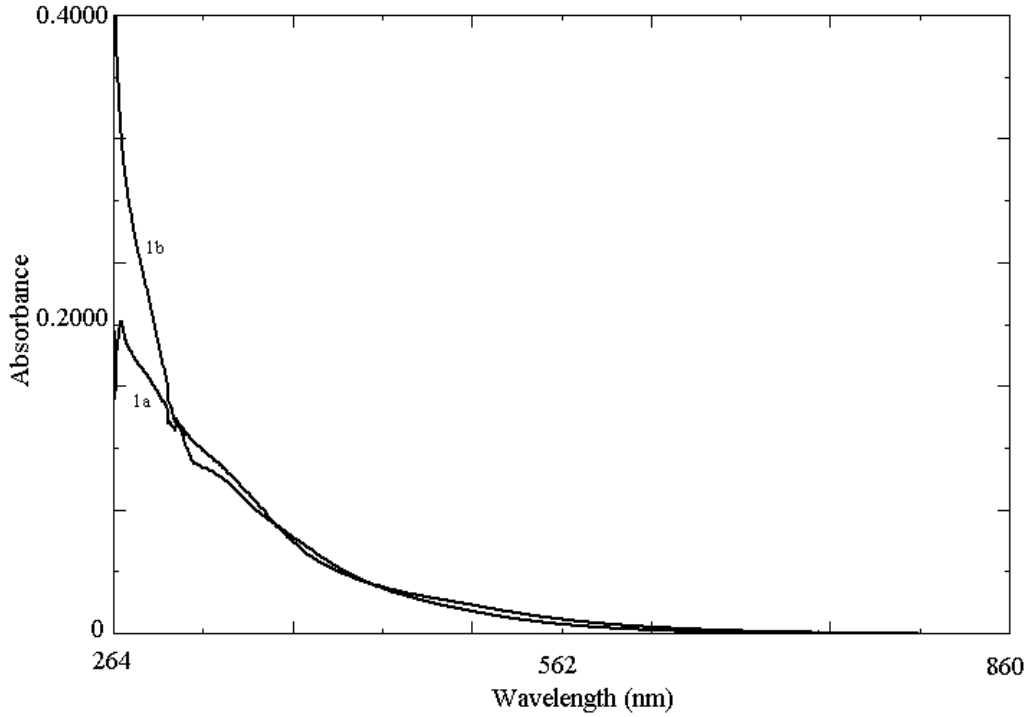

Figure 3.23 Absorption spectra of 1a and 1b in dimethylformamide

Emission spectra of derivatives 1 were recorded in six solvents at the concentration of 5 x 10^{-6} M and they are shown in Figure 3.24 – 3.29.

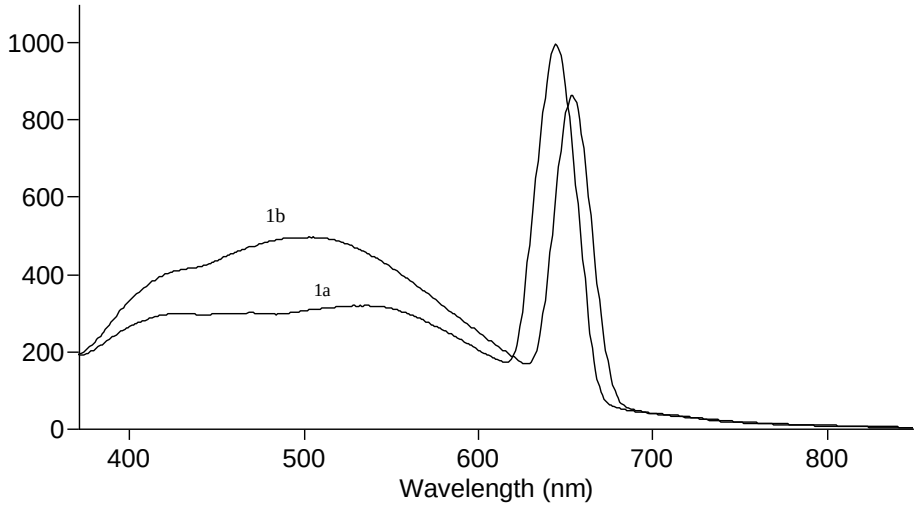

Figure 3.24 Emission spectra of 1a and 1b in toluene

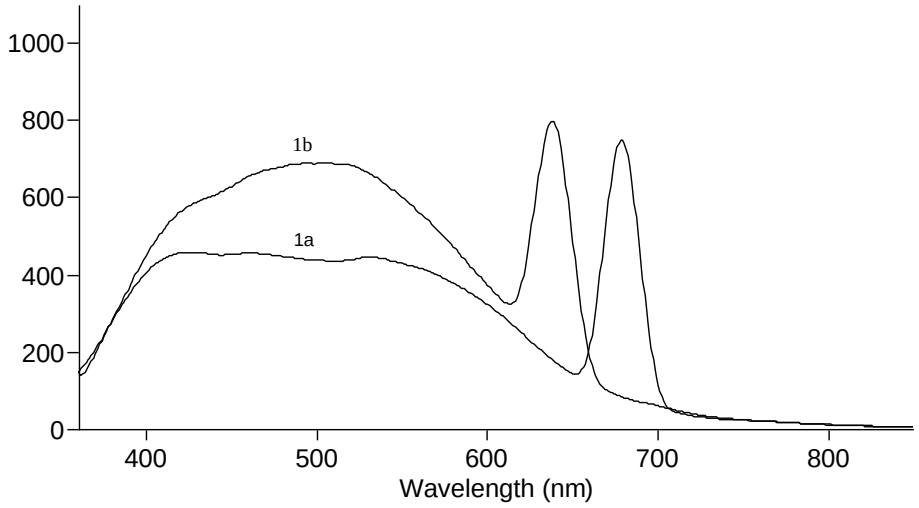

Figure 3.25 Emission spectra of 1a and 1b in dichloromethane

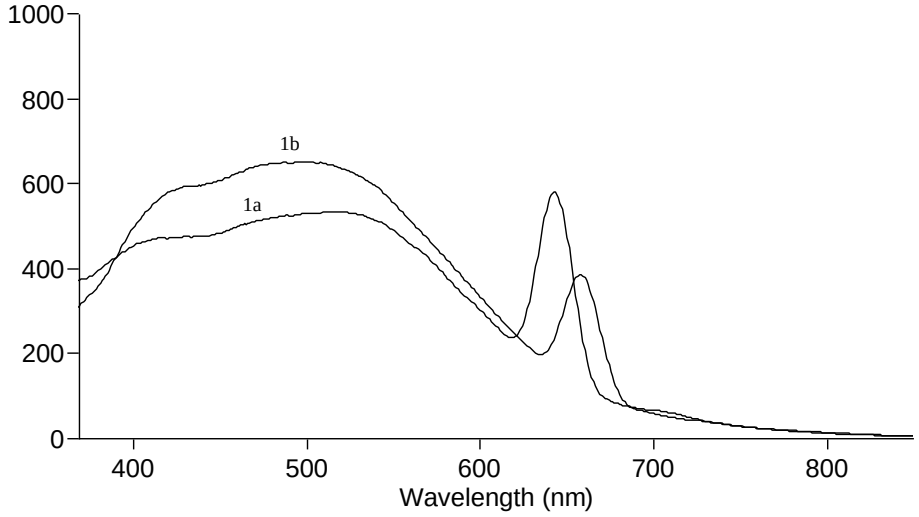

Figure 3.26 Emission spectra of 1a and 1b in tetrahydrofuran

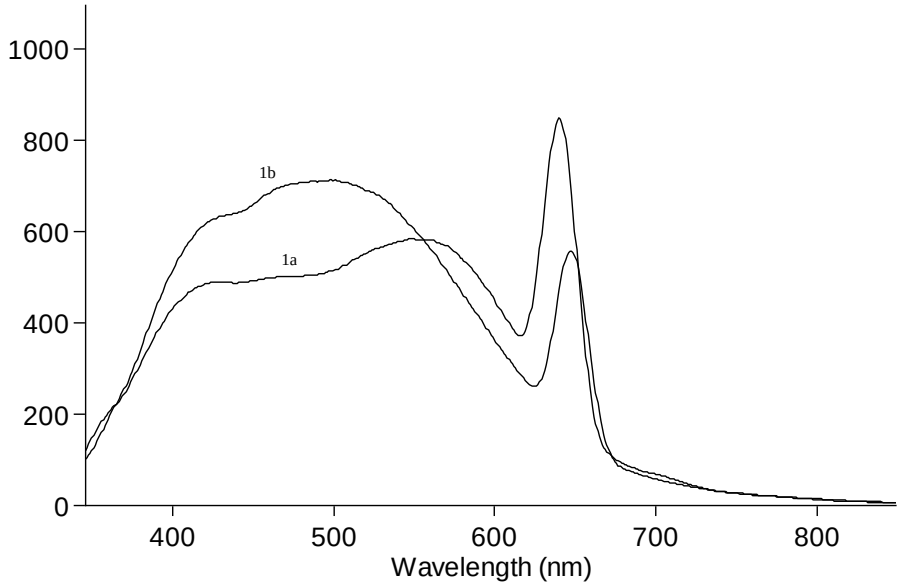

Figure 3.27 Emission spectra of 1a and 1b in ethyl acetate

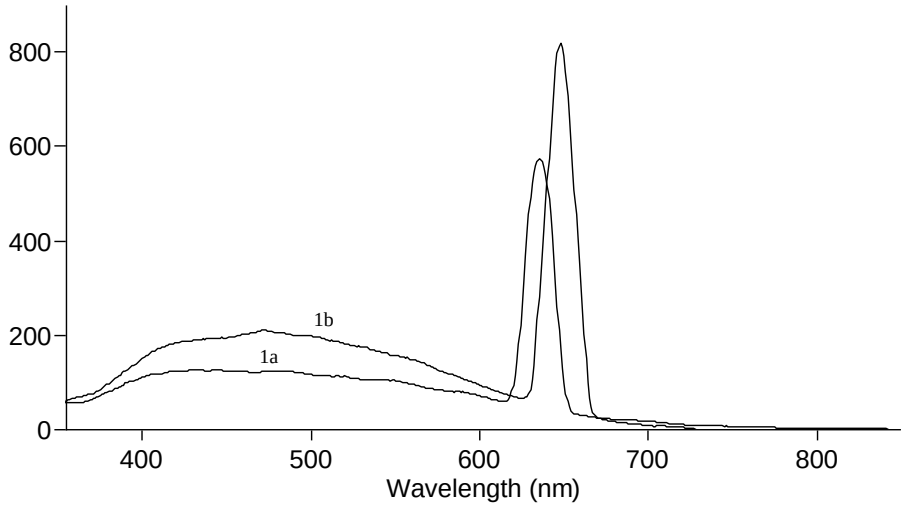

Figure 3.28 Emission spectra of 1a and 1b in acetonitrile

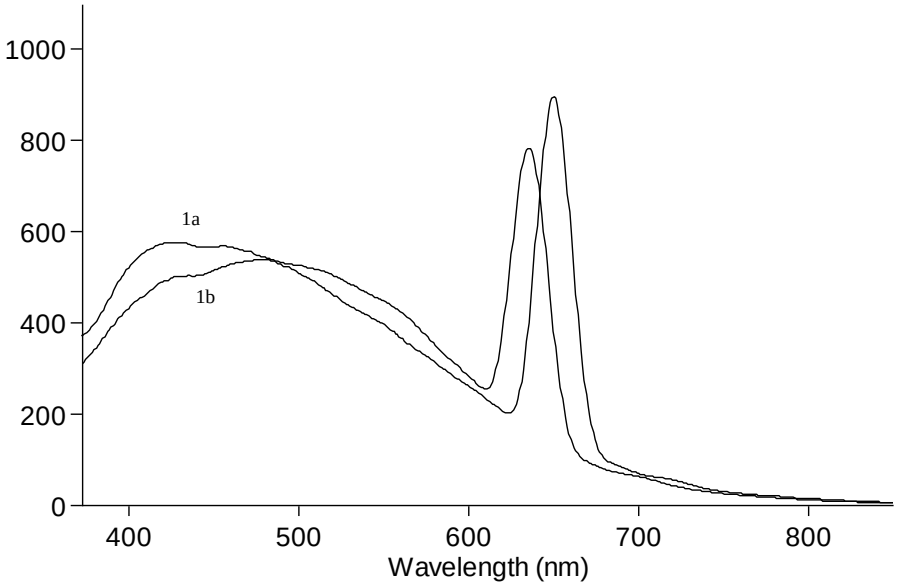

Figure 3.29 Emission spectra of 1a and 1b in dimethylformamide

The photostabilities of derivatives 1a and 1b were recorded in six solvents after 1 h of monitoring and they are shown in Figure 3.30 – 3.41.

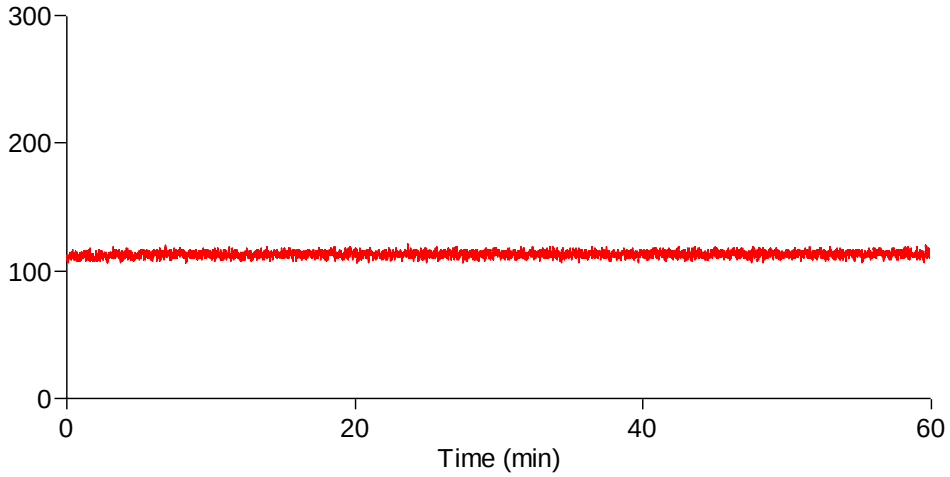

Figure 3.30 The photostability test result of 1a in toluene

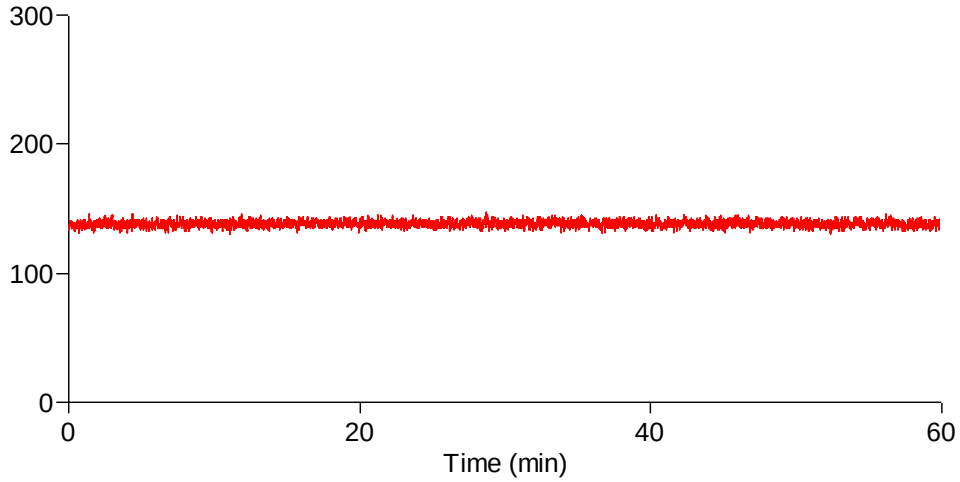

Figure 3.31 The photostability test result of 1a in dichloromethane

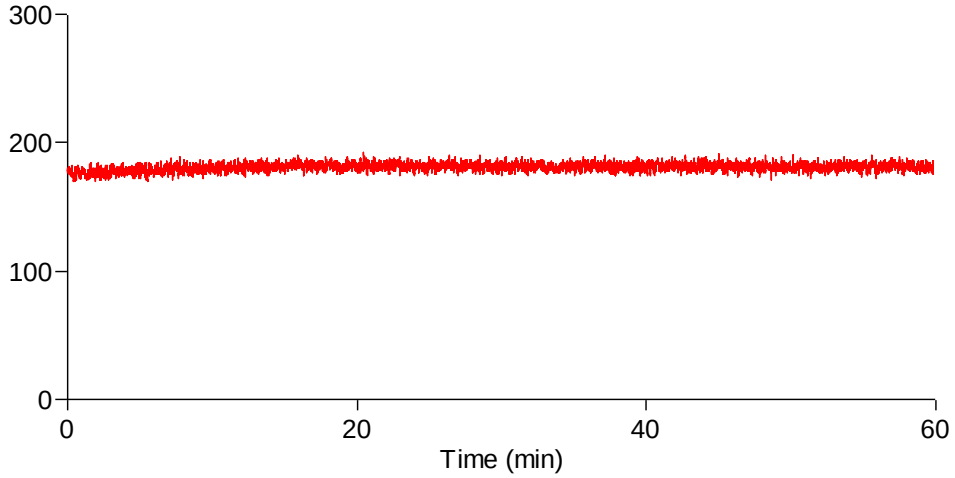

Figure 3.32 The photostability test result of 1a in tetrahydrofuran

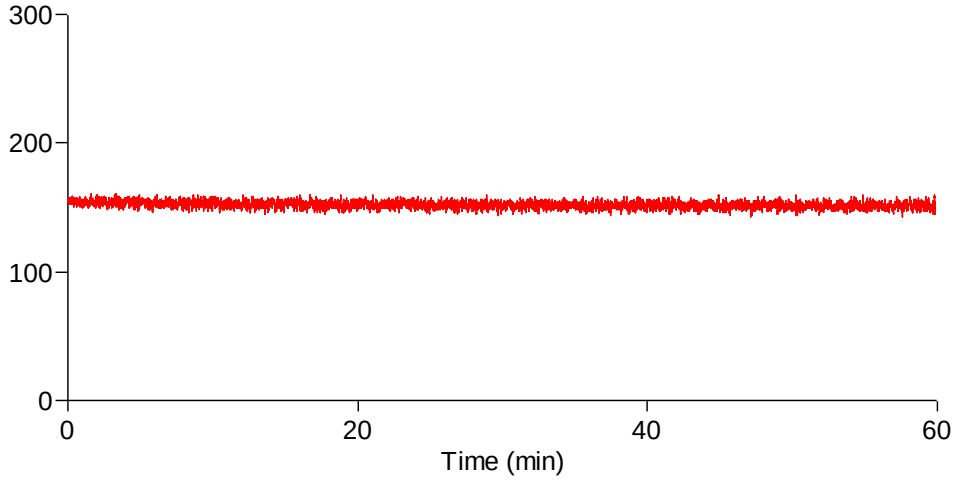

Figure 3.33 The photostability test result of 1a in ethyl acetate

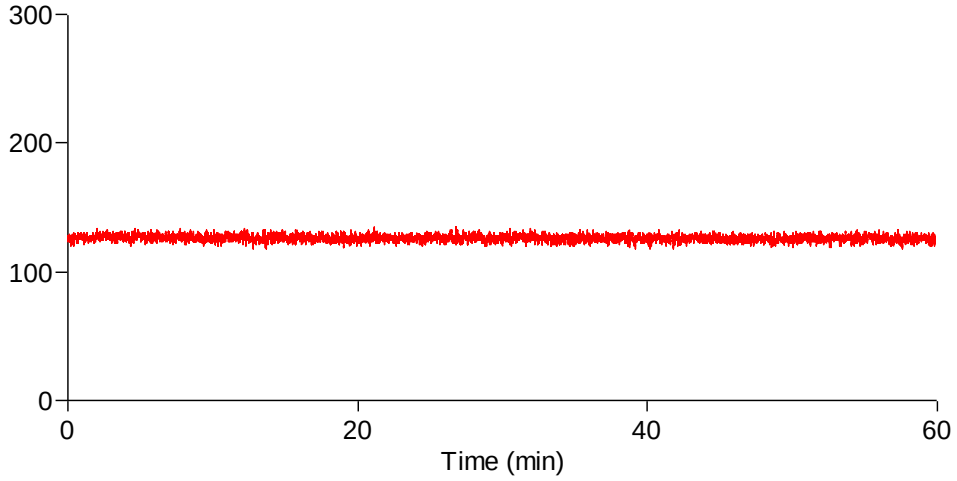

Figure 3.34 The photostability test result of 1a in acetonitrile

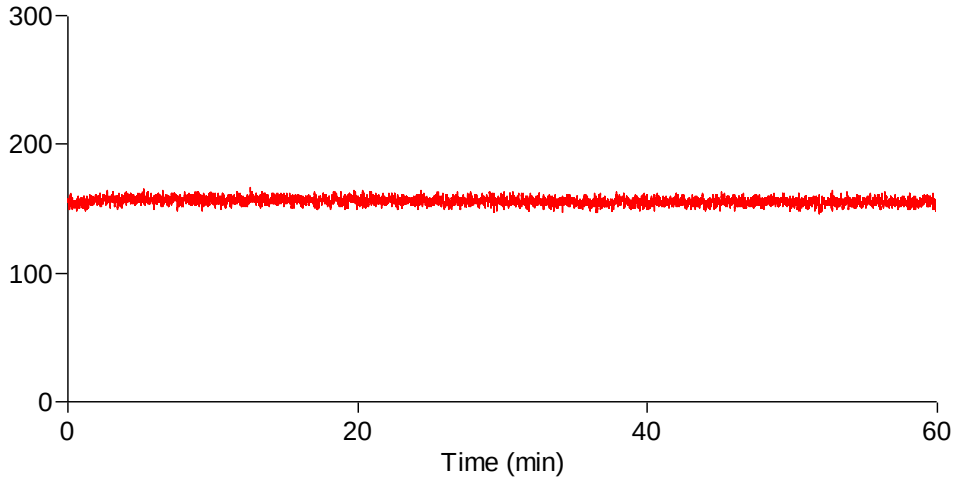

Figure 3.35 The photostability test result of 1a in dimethylformamide

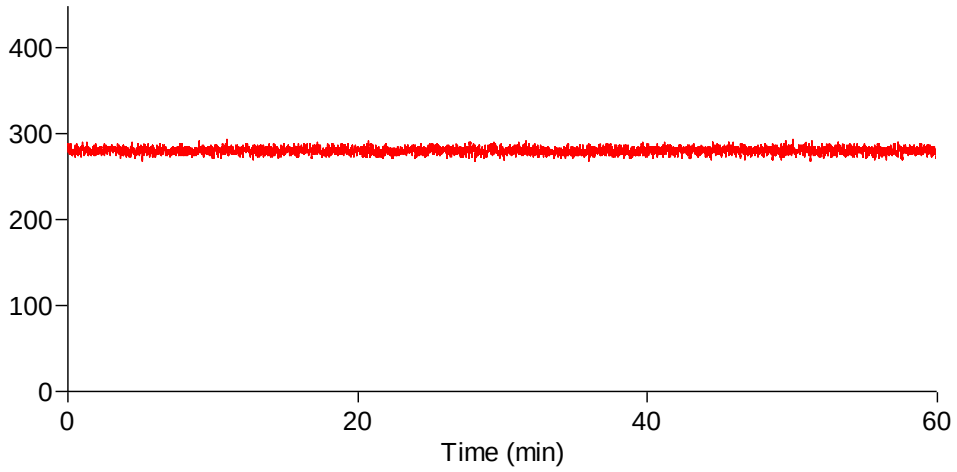

Figure 3.36 The photostability test result of 1b in toluene

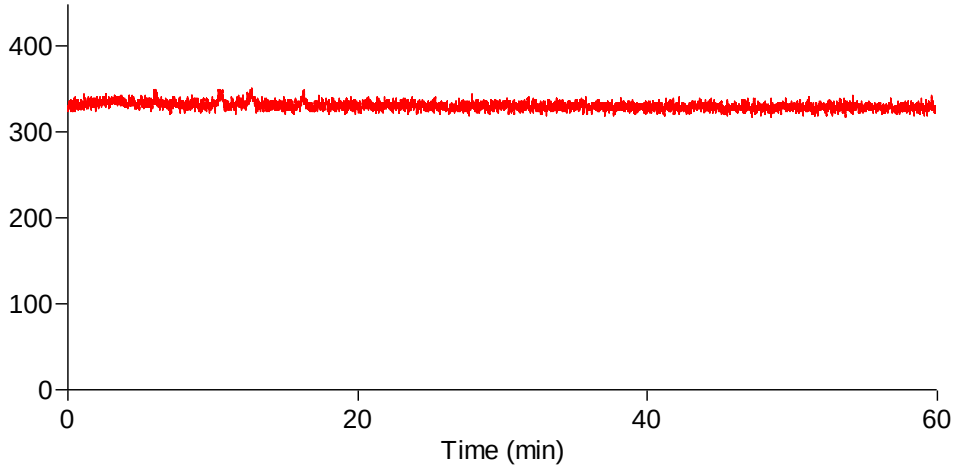

Figure 3.37 The photostability test result of 1b in dichloromethane

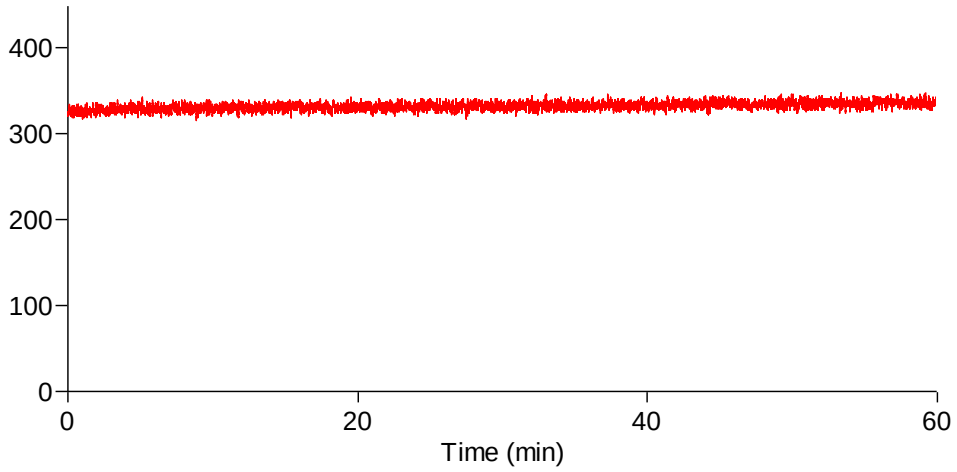

Figure 3.38 The photostability test result of 1b in tetrahydrofuran

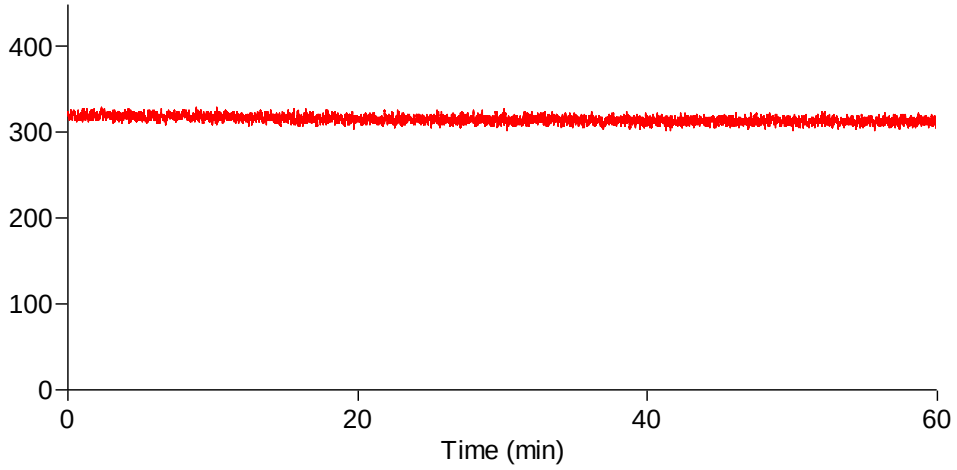

Figure 3.39 The photostability test result of 1b in ethyl acetate

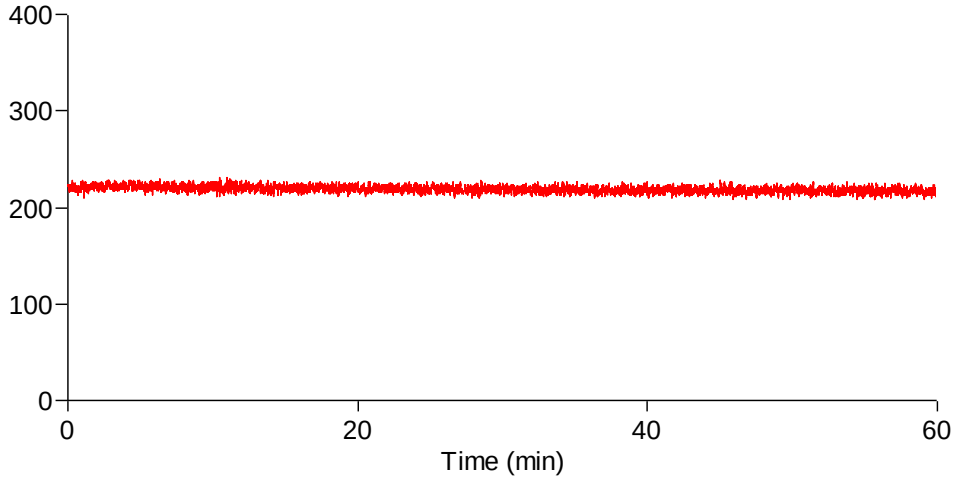

Figure 3.40 The photostability test result of 1b in acetonitrile

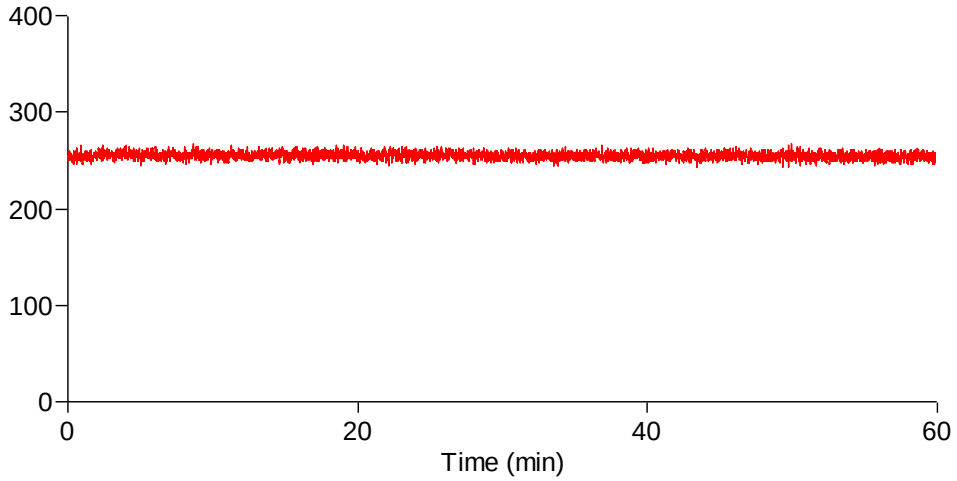

Figure 3.41 The photostability test result of 1b in dimethylformamide

CHAPTER FOUR
CONCLUSION

In this study, the two new Y-shaped fluorophores, 1a and 1b containing an imidazole core and N-phenyl-aza-15-crown-5 have been synthesized as shown in Figure 2.7. The Y-shaped molecules have been synthesized by the Debus reaction between derivatives 2 and 4-formylbenzo-aza-15-crown-5.

The structures of the synthesized compounds were confirmed by FT-IR spectra and ^{1}H-NMR analysis.

The FT-IR data of 1a and 1b were given in Table 3.13 and 3.16, respectively. The FT-IR spectra of 1a and 1b showed that 1a and 1b had the vibration frequencies of the −N−H bands at 3422 cm^{-1} and 3438 cm^{-1}, −C=N bands at 1606 cm^{-1} and 1607 cm^{-1}, −C−N bands at 1246 cm^{-1} and 1250 cm^{-1}, respectively. The −CO bands which were at 1694 cm^{-1}, 1684 cm^{-1}, and 1666 cm^{-1} for 2a, 2b and 4-formylbenzo-aza-15-crown-5, respectively, were not observed at the FT-IR spectra of 1a and 1b. The carbonyl group of aldehyde frequency of 4-formylbenzo-aza-15-crown-5 at 2728 cm^{-1} was also not observed at the FT-IR spectra of 1a and 1b, indicating the formation of derivatives 1.

^{1}H-NMR spectral data of 1a and 1b were recorded in $CDCl_3$. ^{1}H-NMR data of 1a and 1b were given in Table 3.14 and 3.17, respectively. The signals of the imidazole protons (−N−H) were at 12.72 ppm and 12.73 ppm for 1a and 1b, respectively, which are in agreement with the results obtained in the literature. The phenyl and vinyl protons of 1a were in the range of 7.72 – 6.38 ppm as multiplet and the crown ether protons were in the range of 3.82 – 3.35 ppm as multiplet. The phenyl and vinyl protons of 1b appeared at 7.49 – 6.28 ppm as multiplet and the crown ether protons and the methoxy (−OCH_3) protons appeared at 3.98 – 3.13 ppm as multiplet. The aldehyde proton of 4-formylbenzo-(aza-15-crown-5) which was at 9.70 ppm as singlet, was not observed at ^{1}H-NMR spectra of 1a and 1b indicating the formation of the desired structures.

The absorption and emission spectra of derivatives 1 were recorded in six solvents of toluene, dichloromethane, tetrahydrofuran, ethyl acetate, acetonitrile and dimethylformamide with different polarity (Figure 3.18 – 3.29) and the spectral properties are summerized in Table 3.18 and Table 3.19 for 1a and 1b, respectively. Both derivatives exhibited two absorption and emission maxima. The absorption maxima of 1a and 1b were between 262 – 343 nm and 262 – 333 nm, respectively. The emission maxima of 1a and 1b were between 412 – 677 nm and 418 – 657 nm, respectively. 1a had the longest absorption maximum at 343 nm in dichloromethane. The absorption bands are not sensitive to solvent polarity. There was no obvious change in the absorption maxima with increasing solvent polarity. While there was no obvious change in the first and third emission maxima, for the second emission maxima blue shift was observed for both derivatives in acetonitrile and dimethylformamide regarding the increase in solvent polarity. In general, because of having the methoxy goup as an electron donating group which increases the length of the conjugated bridge, 1b exhibited longer absorption maxima and emission maxima and bigger Stokes' shift values than 1a. In general, the stronger donor and / or acceptor group are the smaller energy difference between ground and excited states and the longer wavelength of absorption.

The compounds exhibited moderate Stokes' shift values ranging from 82 to 102 nm for 1a and from 91 to 111 nm for 1b which confers to the advantage of better spectral resolution in emission based studies. The highest Stokes' shift value was obtained for 1b in dichloromethane.

The extinction coefficients at the shorter absorption maxima are higher than the extinction coefficients at the longer absorption maxima for both 1a and 1b in all the solvents tested. The extinction coefficient values of 1b are higher than for 1a.

The fluorescence quantum yields of the compounds were determined by using quinine sulphate as a standart in 0.1 M sulphuric acid. As expected, due to a further extension of the conjugated system, there was an increase in the fluorescence

quantum yield of 1b. The highest quantum yield value was observed for 1b in toluene.

The photostability of 1a and 1b were recorded on a steady–state spectrofluorometer in six different solvents of toluene, dichloromethane, tetrahydrofuran, ethyl acetate, acetonitrile and dimethylformamide after 1 h of monitoring as shown in Figure 3.30 – 3.41. The data were acquired their maximum emission wavelengths. The derivatives 1 showed excellent photostabilities.

REFERENCES

Al-Azzawi, R. W. (2007). *Evaluation of some properties of three types of denture reline materials with miconazole (antifungal agent) preparation*. M.Sc Thesis, Prosthetic Department, University of Baghdad, Iraq.

Bhatnagar, A., Sharma, P. K., & Kumar, N. (2011). A review on "imidazoles": Their chemistry and pharmacological potentials. *International Journal of PharmTech Research, 3*, 268-282.

Boni, L. D., Silva, D. L., Neves, U. M., Feng, K., Meador, M., Bu, X. R., et al. (2005). Two- and three-photon excited fluorescence in Y-shaped molecules. *Chemical Physics Letters, 402* (4-6), 474-478.

Chavis, J. C. (2003). *What is a fluorophore?*. Retrieved May 10, 2014, from http://www.wisegeek.com/what-is-a-fluorophore.htm.

Crouch, R. D., Howard, J. L., Zile, J. L., & Barker, K. H. (2006). Microwave-mediated synthesis of lophine: Developing a mechanism to explain a product. *Journal of Chemical Education, 83* (11), 1658-1660.

Debus, H. (1858). Ueber die einwirkung des ammoniaks auf glyoxal. *Justus Liebigs Annalen der Chemie, 107* (2), 199-208.

Draye, M., Le Buzit, G., Fools, J., Guy, A., Leclere, B., Doutreluingne, P., et al. (1997). A recovery process of strontium from acidic nuclear waste streams. *Separation Science and Technology, 32* (10), 1725-1737.

Elderfield, R. C. (1957). 5-membered heterocycles combining two heteroatoms & their benzo derivatives. *Heterocyclic Compound, 5*, 744.

Fernandez, G. A., & Muñoz de la Peña, A. (1985). *Determination of inorganic substances by luminescence methods.* New York: Wiley & Sons.

Finar, I. L. (2006). *Organic chemistry: Stereochemistry and the chemistry of natural products* (5th ed.). India: Dorling Kindersley.

He, G. S., Tan, L. S., Zheng, Q., & Prasad, P. N. (2008). Multiphoton absorbing materials: Molecular designs, characterizations and applications. *Chemical Reviews, 108* (4), 1245-1330.

Islam, A., Tsou, C. C., Hsu, H. J., Shih, W. L., Liu, C. H., & Cheng, C. H. (2002). Novel blue fluorescent dopants based on imidazole-containing compound for organic electroluminescent devices. *Tamkang Journal of Science and Engineering, 5* (2), 69-80.

Jayabharathi, J., Thanikachalam, V., Devi, K. B., & Srinivasan, N. (2011). Physicochemical studies of some novel Y-shaped imidazole derivatives – A sensitive chemisensor. *Spectrochimica Acta Part A: Molecular and Biomolecular Spectroscopy, 82*, 513-520.

Jayabharathi, J., Thanikachalam, V., Srinivasan, N., & Jayamoorthy, K. (2011). Physicochemical studies of bioactive heterocycles of some novel imidazole derivatives as sensitive NLO materials. *Spectrochimica Acta Part A: Molecular and Biomolecular Spectroscopy, 83*, 329-336.

Karunakaran, C., Jayabharathi, J., Jayamoorthy, K., & Devi, K. B. (2012). Sensing rutile TiO_2 through fluorescence of imidazole derivative. *Sensors and Actuators B: Chemical, 168*, 263-270.

Kim, M. S., Ju, J. J., Park, S. K., Do, J. Y., & Lee, M. H. (2008). Cascaded wavelength conversion as favorable application of nonlinear optical polymers. *Optics Express, 16* (13), 9726-9738.

Lakowicz, J. R. (1999). *Principles of fluorescence spectroscopy* (2nd ed.). New York: Kluwer Academic / Plenum Publishers.

Mateeva, N., Deligeorgiev, T., Mitewa, M., & Simova S. (1992). Styryl dyes containing an aza-15-crown-5 macroheterocycle moiety. *Dyes and Pigments, 20* (4), 271-278.

Minkin, V. I., Dubonosov, A. D., Bren, V. A., & Tsukanov, A. V. (2008). Chemosensors with crown ether based receptors. *Archive for Organic Chemistry,* (4), 90-102.

Ozturk, G., Alp, S., & Ergun, Y. (2007). Synthesis and spectroscopic properties of new 5-oxazolone derivatives containing an *N*-phenyl-aza-15-crown-5 moiety. *Tetrahedron Letters, 48* (41), 7347-7350.

Ozturk, G., Karakas, D., Karadag, F., & Yorgun, C. (2012). Synthesis and characterization of new Y-shaped fluorophores with an imidazole core. *Journal of Fluorescence, 22* (4), 1159-1164.

Pedersen, C. J. (1967). Cyclic polyethers and their complexes with metal salts. *Journal of the American Chemical Society, 89* (26), 7017-7036.

Pond, S. J. K., Tsutsumi, O., Rumi, M., Kwon, O., Zojer, E., Brédas, J. L., et al. (2004). Metal-ion sensing fluorophores with large two-photon absorption cross sections: Aza-crown ether substituted donor–acceptor–donor distyrylbenzenes. *Journal of the American Chemical Society, 126* (30), 9291-9306.

Ren, J., Wang, S. M., Wu, L. F., Xu, Z. X., & Dong, B. H. (2008). Synthesis and properties of novel Y-shaped NLO molecules containing thiazole and imidazole chromophores. *Dyes and Pigments, 76* (2), 310-314.

Renouard, T., Fallahpour, R. A., Nazeeruddin, M. K., Humphry-Baker, R., Gorelsky, S. I., Lever, A. B. P., et al. (2002). Novel ruthenium sensitizers containing functionalized hybrid tetradentate ligands: Synthesis, characterization, and INDO/S analysis. *Inorganic Chemistry, 41* (2), 367-378.

Santos, J., Mintz, E. A., Zehnder, O., Bosshard, C., Bu, X. R., & Günter, P. (2001). New class of imidazoles incorporated with thiophenevinyl conjugation pathway for robust nonlinear optical chromophores. *Tetrahedron Letters, 42* (5), 805-808.

Saravanan, K., Srinivasan, N., Thanikachalam, V., & Jayabharathi, J. (2011). Synthesis and photophysics of some novel imidazole derivatives used as sensitive fluorescent chemisensors. *Journal of Fluorescence, 21*, 65-80.

Shalini, K., Sharma, P. K., & Kumar, N. (2010). Imidazole and its biological activities: A review. *Der Chemica Sinica, 1* (3), 36-47.

Shi, R., Pan, Q., Guan, Y., Hua, Z., Huang, Y., Zhao, M., et al. (2007). Imidazole as a catalyst for in vitro refolding of enhanced green fluorescent protein. *Archives of Biochemistry and Biophysics, 459*, 122-128.

Skoog, D. A., Holler, F. J., & Nieman, T. A. (1998). *Principles of instrumental analysis* (5th ed.). The United States of America: Harcourt Brace & Company.

Steed, J. W. (2001). First- and second-sphere coordination chemistry of alkali metal crown ether complexes. *Coordination Chemistry Reviews, 215*, 171-221.

Uçucu, U., Karaburun, N. G., & Işikdağ, I. (2001). Synthesis and analgesic activity of some 1-benzyl-2-substituted-4,5-diphenyl-1H-imidazole derivatives. *IL Farmaco, 56* (4), 285-290.

Valeur, B. (2002). *Molecular fluorescence principles and applications*. Weinheim: Wiley-VCH.

Wang, S., Zhao, L., Xu, Z., Wu, C., & Cheng, S. (2002). Novel nonlinearity-transparency-thermal stability trade-off of imidazole chromophores for nonlinear optical application. *Materials Letters, 56* (6), 1035-1038.

Yu, J. M., Chen, C. Y., & Chen, Y. (2011). Synthesis and fluorescent sensory properties of a 5-cyanostilbene derivative linked to monoaza-15-crown-5. *Journal of the Taiwan Institute of Chemical Engineers, 42* (4), 674-681.

Zhang, M., Li, M., Li, F., Cheng, Y., Zhang, J., Yi, T., et al. (2008). A novel Y-type, two-photon active fluorophore: Synthesis and application in ratiometric fluorescent sensor for fluoride anion. *Dyes and Pigments, 77* (2), 408-414.

Zhang, M., Li, M., Zhao, Q., Li, F., Zhang, D., Zhang, J., et al. (2007). Novel Y-type two-photon active fluorophore: synthesis and application in fluorescent sensor for cysteine and homocysteine. *Tetrahedron Letters, 48* (13), 2329-2333.

Zhao, Q., Liu, S., Shi, M., Li, F., Jing, H., Yi, T., et al. (2007). Tuning photophysical and electrochemical properties of cationic iridium (III) complex salts with imidazolyl substituents by proton and anions. *Organometallics, 26* (24), 5922-5930.